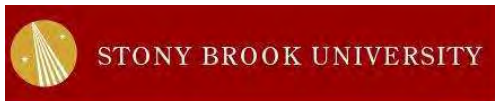


Neutron Star Structure and Measurements

J. M. Lattimer

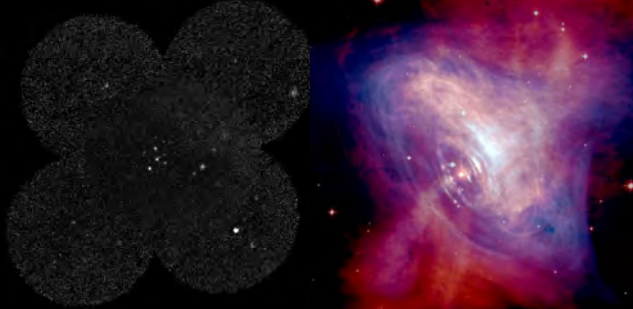
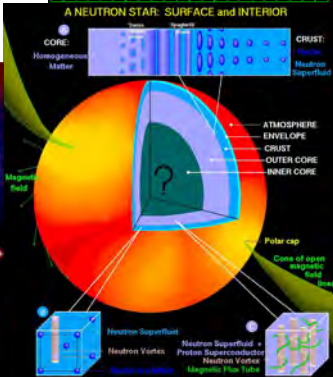
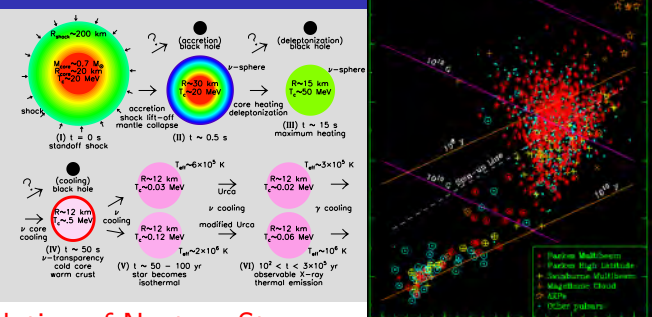
Department of Physics & Astronomy



N3AS 2024 Santa Cruz Summer School
UC Santa Cruz, 13-22 July 2024

Outline

- ▶ Neutron Star Structure
- ▶ Dense Matter Equation of State
- ▶ Nuclear Experimental Constraints
- ▶ Formation and Evolution of Neutron Stars
- ▶ Observational Constraints



Neutron Stars and Extremes

- Highest densities and pressures except for black hole interiors and in the very early universe

The maximum central density of any neutron star (NS) is about 1.5 baryons fm^{-3} or $3 \times 10^{15} \text{ g cm}^{-3}$. One teaspoon on Earth would weigh as much as 7 million elephants. The maximum central pressure is 1 GeV fm^{-3} or $1.6 \times 10^{29} \text{ atm}$.

- Largest surface gravity: $10^{14} \text{ cm s}^{-2}$ or 100 billion Earth's gravities.

- Highest inferred magnetic fields, $\sim 10^{15} \text{ G}$.

Those NSs with $B \gtrsim 10^{14} \text{ G}$ are known as magnetars, and are powered by magnetic field decay rather than spin-down.

- Highest temperature matter except for black hole formation

A newly born NS has an interior temperature as high as $k_B T = 100 \text{ MeV}$ or $T = 10^{12} \text{ K}$.

- Highest temperature superfluid, $T_c = 10^9 \text{ K}$ (Cas A).

- Fastest spinning macroscopic object, 716Hz (PSR J1748-2446ad).

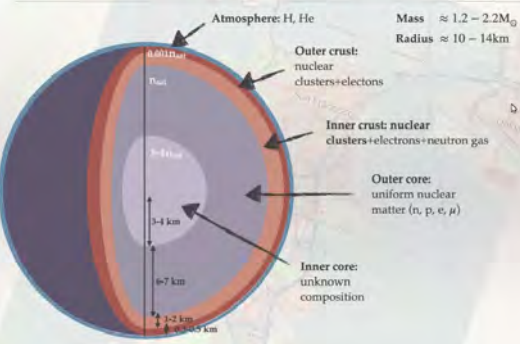
Surface equatorial velocity $\sim c/4$.

- Highest stellar spatial velocity, $0.01c$ (IGR J11014-6103).

- Only place in universe where neutrinos can be temporarily trapped.

Neutron Stars: The Basics

- Nearly all known NSs are pulsars (rapidly rotating and highly magnetized) that emit X-ray, optical or radio beams from their poles, like a lighthouse.
- The radii of most NSs are about 12 km.



- The predominant component of NSs are.....**neutrons!**
- Most, if not all, NSs are formed in the gravitational collapse of massive stars at the ends of their lives; some of those collapses produce black holes instead. Some massive NSs may be formed in the aftermath of a binary merger of two lower-massed neutron stars.
- The minimum possible NS mass is $0.1M_{\odot}$, but none are observed to be less massive than $1M_{\odot}$.
- The maximum possible NS mass is less than $2.5M_{\odot}$, and the largest observed mass is 2.08 ± 0.07 (PSR J0437-4715).

Neutron Stars: History

- 1920** Rutherford predicts the neutron
- 1931** Landau *anticipates* single-nucleus stars but not neutron stars
- 1932** Chadwick discovers the neutron
- 1934** W. Baade and F. Zwicky predict existence of neutron stars as end products of supernovae
- 1939** Oppenheimer and Volkoff predict upper mass limit of neutron star.
- 1964** Hoyle, Narlikar and Wheeler predict neutron stars rapidly rotate
- 1965** Hewish and Okoye discover intense radio source in Crab nebula
- 1966** Colgate and White perform simulations of supernovae leading to neutron stars.
- 1967** C. Schisler discovers a dozen pulsing radio sources, including the Crab pulsar, using secret military radar in Alaska. X-1.
- 1967** Hewish, Bell, Pilkington, Scott and Collins discover “first” PSR 1919+21, Aug 6.
- 1968** The Crab Nebula pulsar is discovered, found to be slowing down (ruling out binary and vibrational models), and clinched the connection to supernovae.
- 1968** The term “pulsar” first appears in print, in the *Daily Telegraph*.
- 1969** “Glitches” observed; evidence for superfluidity in neutron star crust.

- 1971** Accretion powered X-ray pulsar discovered by Uhuru (*not* the Lt.)
- 1974** Hewish awarded Nobel Prize (but Bell and Okoye were not)
- 1974** Lattimer and Schramm predict merger mass ejection and r-process
- 1974** Binary pulsar PSR 1913+16 discovered by Hulse and Taylor.
orbital decay due to GR gravitational radiation
- 1979** Chart recording of PSR 1919+21 used as album cover for *Unknown Pleasures* by Joy Division (#19/100 greatest British album).
- 1982** First millisecond pulsar, PSR B1937+21,
discovered by Backer et al. at Arecibo.
- 1992** Discovery of first extra-solar planets
orbiting PSR B1257+12 by Wolszczan and Frail.
- 1993** Hulse and Taylor receive Nobel Prize
- 1998** Kouveliotou et al. discover first magnetar
- 2004** SGR 1806-20: largest burst of energy seen
in Galaxy since SN 1604, brighter than Moon in
 γ rays, more energetic than L_\odot for 100,000 years
- 2004** Hessels et al. discover PSR J1748-2446ad;
fastest rotation rate, 716 Hz.
- 2005** Hessels et al. discover PSR J0737-3039, first two-pulsar binary
- 2013** Stairs et al. find first pulsar in triple system
- 2013** Antoniadis et al. find first $2M_\odot$ pulsar
- 2017** GW170817: first detected neutron star merger, r-process evidence



sleevage.com/joy-division-unknown-pleasures/

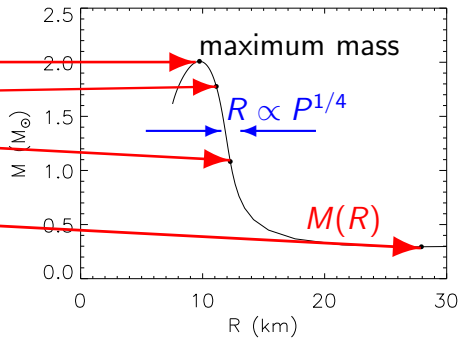
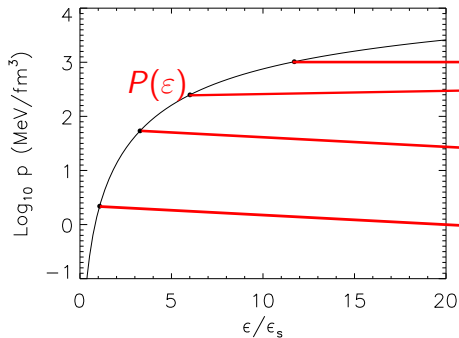
Important Questions

- ▶ How Does the Structure of Neutron Stars Depend On the Nucleon-Nucleon Interaction?
 - ▶ The Neutron Star Maximum Mass and Causality
 - ▶ The Neutron Star Radius and the Nuclear Symmetry Energy
 - ▶ Does Exotic Matter (Hyperons, Kaons/Pions, Deconfined Quarks) Exist in Neutron Star Interiors?
- ▶ How Do Nuclear Experiments Constrain the Nuclear Symmetry Energy and Neutron Star Radii?
 - ▶ Binding Energies
 - ▶ Heavy ion Collisions
 - ▶ Neutron Skin Thicknesses
 - ▶ Dipole Polarizabilities
 - ▶ Giant (and Pygmy) Dipole Resonances
 - ▶ Pure Neutron Matter
- ▶ What Astrophysical Constraints Exist?
 - ▶ Nuclear Mass Measurements
 - ▶ Photospheric Radius Expansion Bursts
 - ▶ Thermal Emission from Isolated and Quiescent Binary Sources
 - ▶ Pulse Profile Modeling of X-ray Pulsars, QPOs from Accretion, etc.

Neutron Star Structure

Tolman-Oppenheimer-Volkov equations

$$\frac{dP}{dr} = -\frac{G}{c^2} \frac{(m + 4\pi pr^3/c^2)(\varepsilon + P)}{r(r - 2Gm/c^2)}$$
$$\frac{dm}{dr} = 4\pi \frac{\varepsilon}{c^2} r^2$$



Equation of State

Observations

Mass-Radius Diagram and Theoretical Constraints

GR:

$$R > 2GM/c^2$$

$P < \infty$:

$$R > (9/4)GM/c^2$$

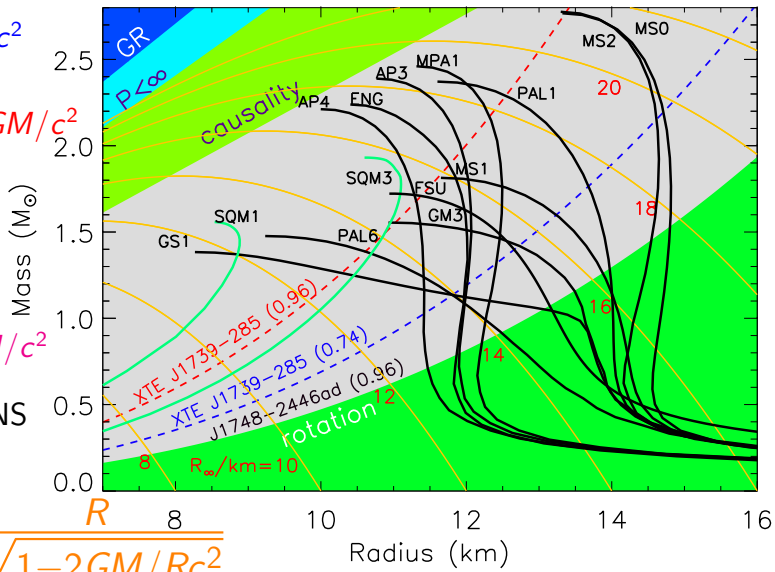
causality:

$$R \gtrsim 2.9GM/c^2$$

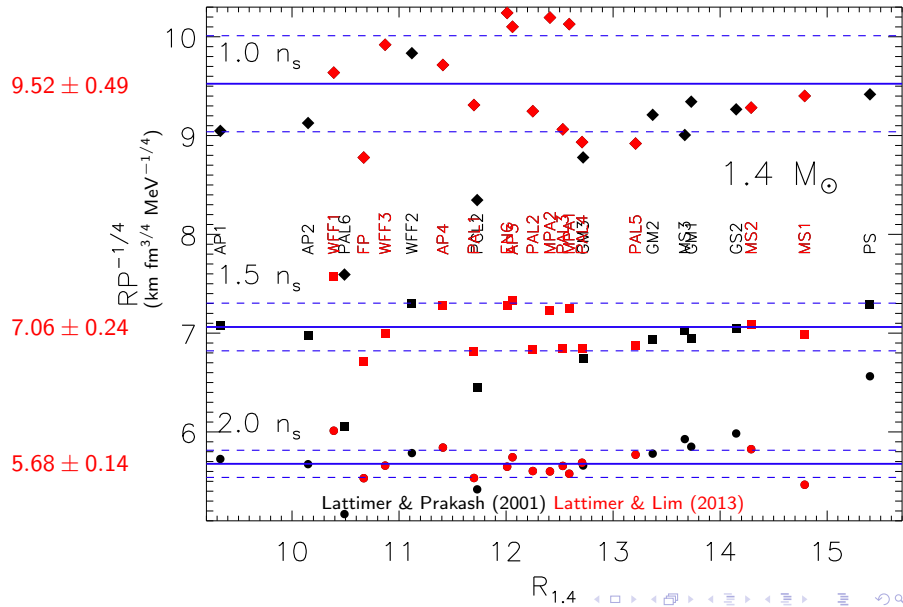
— normal NS

— SQS

$$R_\infty = \frac{R}{\sqrt{1 - 2GM/Rc^2}}$$



The Radius – Pressure Correlation



Neutron Star Structure

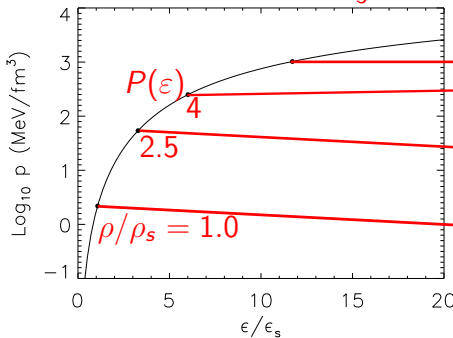
Newtonian Gravity:

$$\frac{dP}{dr} = -\frac{Gm\rho}{r^2}; \quad \frac{dm}{dr} = 4\pi\rho r^2; \quad \rho c^2 = \epsilon$$

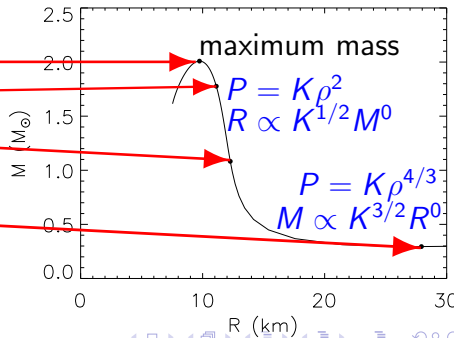
Newtonian Polytrope:

$$P = K\rho^\gamma; \quad M \propto K^{1/(2-\gamma)} R^{(4-3\gamma)/(2-\gamma)}$$

$$\rho < \rho_s: \gamma \simeq \frac{4}{3};$$

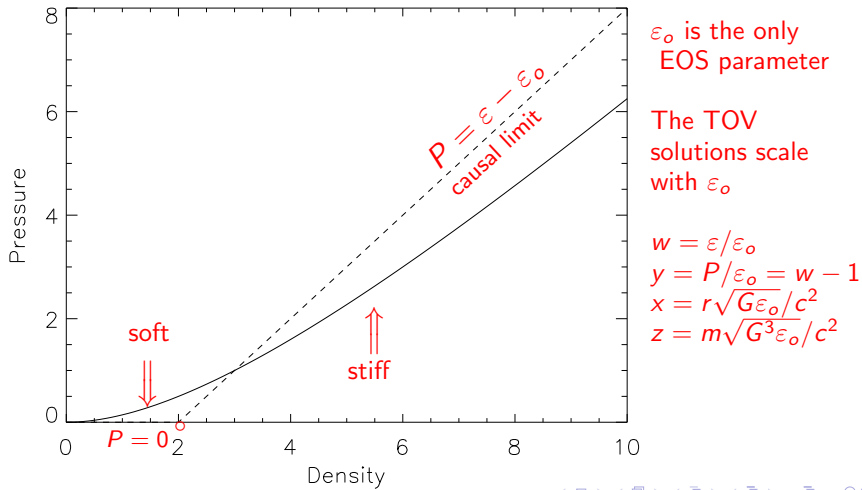


$$\rho > \rho_s: \gamma \simeq 2$$



Extremal Properties of Neutron Stars

- The most compact and massive configurations occur when the low-density equation of state is "soft" and the high-density equation of state is "stiff" (Koranda, Stergioulas & Friedman 1997).



Extremal Properties of Neutron Stars

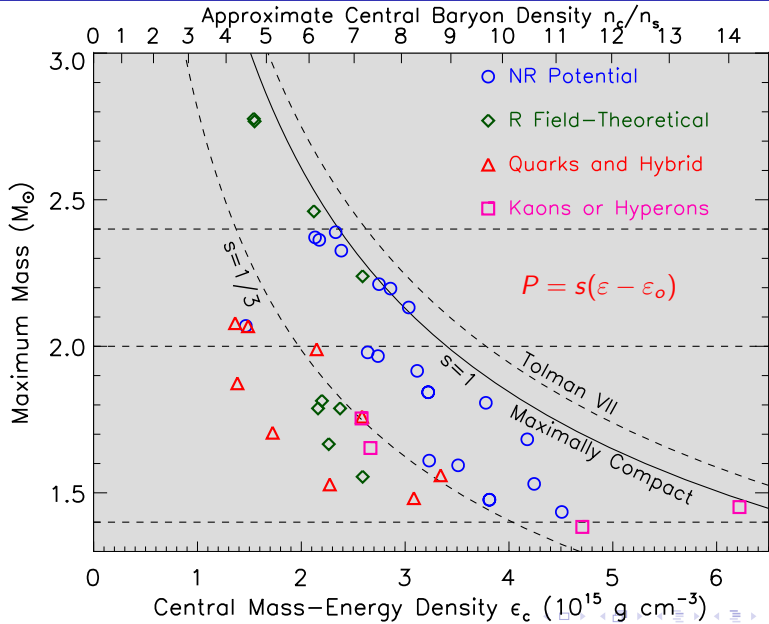
The maximum mass configuration is achieved when
 $x_R = 0.2404$, $w_c = 3.034$, $y_c = 2.034$, $z_R = 0.08513$.

A useful reference density is the nuclear saturation density
(interior density of normal nuclei):

$$\rho_s = 2.7 \times 10^{14} \text{ g cm}^{-3}, n_s = 0.16 \text{ baryons fm}^{-3}, \varepsilon_s = 150 \text{ MeV fm}^{-3}$$

- ▶ $M_{\max} = 4.1 (\varepsilon_s/\varepsilon_o)^{1/2} M_\odot$ (Rhoades & Ruffini 1974)
- ▶ $M_{B,\max} = 5.41 (m_B c^2/\mu_o)(\varepsilon_s/\varepsilon_o)^{1/2} M_\odot$
- ▶ $R_{\min} = 2.82 GM/c^2 = 4.3 (M/M_\odot) \text{ km}$
- ▶ $\mu_{b,\max} = 2.09 \text{ GeV}$
- ▶ $\varepsilon_{c,\max} = 3.034 \varepsilon_o \simeq 51 (M_\odot/M_{\text{largest}})^2 \varepsilon_s$
- ▶ $P_{c,\max} = 2.034 \varepsilon_o \simeq 34 (M_\odot/M_{\text{largest}})^2 \varepsilon_s$
- ▶ $n_{B,\max} \simeq 38 (M_\odot/M_{\text{largest}})^2 n_s$
- ▶ $\text{BE}_{\max} = 0.34 M$
- ▶ $P_{\text{spin,min}} = 0.74 (M_\odot/M_{\text{sph}})^{1/2} (R_{\text{sph}}/10 \text{ km})^{3/2} \text{ ms} = 0.20 (M_{\text{sph,max}}/M_\odot) \text{ ms}$

Maximum Energy Density in Neutron Stars



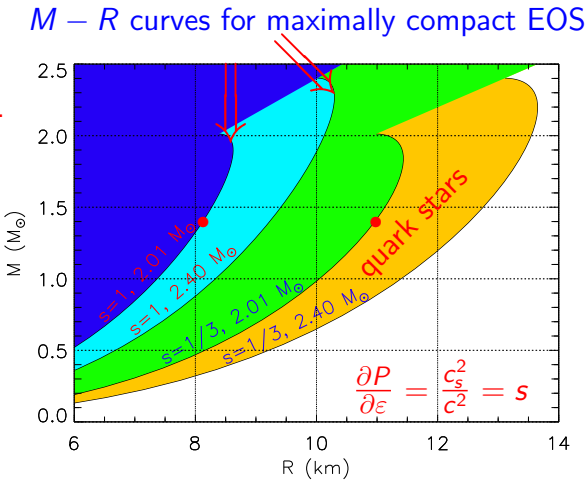
Causality + GR Limits and the Maximum Mass

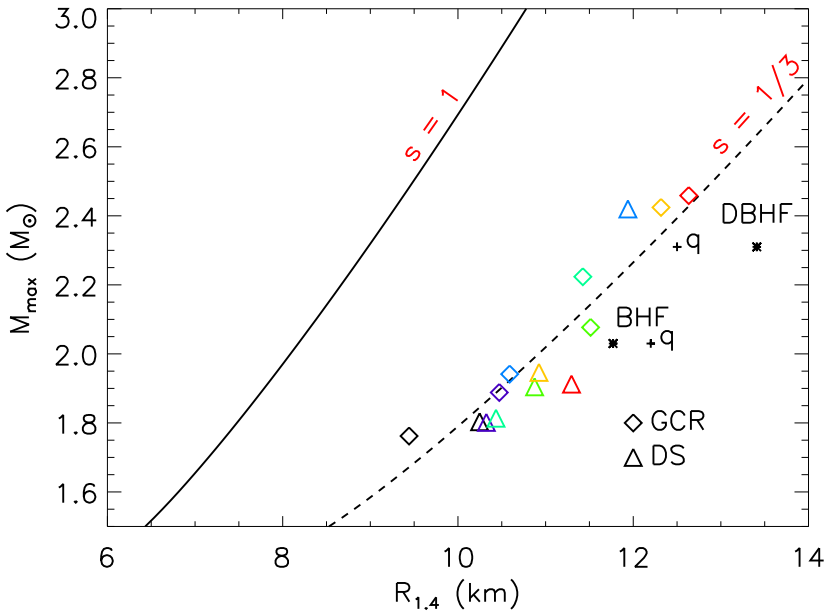
A lower limit to the maximum mass sets a lower limit to the radius for a given mass.

Similarly, a precise (M, R) measurement sets an upper limit to the maximum mass.

$1.4M_{\odot}$ stars must have $R > 8.15M_{\odot}$.

$1.4M_{\odot}$ strange quark matter stars (and likely hybrid quark/hadron stars) must have $R > 11$ km.





Spherically Symmetric General Relativity

Static metric:

$$ds^2 = e^{\lambda(r)} dr^2 + r^2 (d\theta^2 + \sin^2 \theta d\phi^2) - e^{\nu(r)} dt^2$$

Einstein's equations:

$$\begin{aligned} 8\pi\varepsilon(r)Gr^2/c^4 &= 1 - e^{-\lambda(r)} + re^{-\lambda(r)}\lambda'(r), \\ 8\pi P(r)Gr^2/c^4 &= e^{-\lambda(r)} - 1 + re^{-\lambda(r)}\nu'(r), \\ P'(r) &= -\frac{P(r) + \varepsilon(r)}{2}\nu'(r). \end{aligned}$$

Mass: $m(r)c^2 = 4\pi \int_0^r \varepsilon(r')r'^2 dr'$, $e^{-\lambda(r)} = 1 - 2Gm(r)/(rc^2)$

Boundaries:

$$r = 0 \quad m(0) = P'(0) = \varepsilon'(0) = 0,$$

$$r = R \quad m(R) = M, \quad P(R) = 0, \quad e^{\nu(R)} = e^{-\lambda(R)} = 1 - 2GM/(Rc^2)$$

Thermodynamics:

$$\begin{aligned} \frac{dn}{n} &= \frac{d\varepsilon}{\varepsilon + P} = -\frac{d\varepsilon}{dP} \frac{d\nu}{2}, \quad \mu = \frac{d\varepsilon}{dn}, \quad \frac{\varepsilon}{n} = m_b c^2 + e, \quad \frac{P}{n^2} = \frac{de}{dn} \\ m_b c^2 n(r) &= (\varepsilon(r) + P(r))e^{(\nu(r)-\nu(R))/2} - n(R)e(R) \\ N &= \int_0^R 4\pi r^2 e^{\lambda(r)/2} n(r) dr; \quad BE = (Nm_b - M)c^2 \end{aligned}$$

Neutron Star Structure

Tolman-Oppenheimer-Volkov equations of relativistic hydrostatic equilibrium:

$$\frac{dP}{dr} = -\frac{G}{c^2} \frac{(m + 4\pi r^3 P/c^2)(\varepsilon + P)}{r(r - 2Gm/c^2)}$$
$$\frac{dm}{dr} = 4\pi \frac{\varepsilon}{c^2} r^2$$

P is pressure, ε is mass-energy density

Useful analytic solutions exist:

- ▶ Uniform density $\varepsilon = \text{constant}$
- ▶ Tolman VII $\varepsilon = \varepsilon_c [1 - (r/R)^2]$
- ▶ Buchdahl $\varepsilon = \sqrt{PP_*} - 5P$

Uniform Density Fluid

$$\begin{aligned}m(r) &= \frac{4\pi}{3} \frac{\varepsilon}{c^2} r^3 = Mx^{3/2}, & x \equiv \left(\frac{r}{R}\right)^2, & \beta \equiv \frac{GM}{Rc^2} \\e^{-\lambda(r)} &= 1 - 2\beta x, \\e^{\nu(r)} &= \left[\frac{3}{2} \sqrt{1 - 2\beta} - \frac{1}{2} \sqrt{1 - 2\beta x} \right]^2, \\P(r) &= \varepsilon \left[\frac{\sqrt{1 - 2\beta x} - \sqrt{1 - 2\beta}}{3\sqrt{1 - 2\beta} - \sqrt{1 - 2\beta x}} \right], \\ \varepsilon(r) &= \text{constant}; \quad n(r) = \text{constant} \\ \frac{\text{BE}}{Mc^2} &= \frac{3}{4\beta} \left(\frac{\sin^{-1} \sqrt{2\beta}}{\sqrt{2\beta}} - \sqrt{1 - 2\beta} \right) \simeq \frac{3\beta}{5} + \frac{9}{14}\beta^2 + \dots, \\c_s^2 &= \infty\end{aligned}$$

$$P_c < \infty \implies \beta < 4/9$$

$$P_c < \varepsilon \implies \beta < 3/8$$

Tolman VII

$$\varepsilon(r) = \varepsilon_c [1 - (r/R)^2] \equiv \varepsilon_c[1 - x]$$

$$e^{-\lambda(r)} = 1 - \beta x(5 - 3x)$$

$$e^{\nu(r)} = (1 - 5\beta/3) \cos^2 \phi,$$

$$P(r) = \frac{c^2}{4\pi GR^2} \left[\sqrt{3\beta e^{-\lambda(r)}} \tan \phi(r) - \frac{\beta}{2}(5 - 3x) \right],$$

$$n(r) = \frac{\varepsilon(r) + p(r)}{m_b c^2} \frac{\cos \phi(r)}{\cos \phi_1}$$

$$\phi(r) = \frac{w_1 - w(r)}{2} + \phi_1, \quad \phi_1 = \phi(x=1) = \tan^{-1} \sqrt{\frac{\beta}{3(1-2\beta)}},$$

$$w(r) = \ln \left[x - \frac{5}{6} + \sqrt{\frac{e^{-\lambda(r)}}{3\beta}} \right], \quad w_1 = w(x=1) = \ln \left[\frac{1}{6} + \sqrt{\frac{1-2\beta}{3\beta}} \right].$$

$$(P/\varepsilon)_c = \frac{2 \tan \phi_c}{15} \sqrt{\frac{3}{\beta}} - \frac{1}{3}, \quad c_{s,c}^2 = \tan \phi_c \left(\frac{1}{5} \tan \phi_c + \sqrt{\frac{\beta}{3}} \right)$$

$$\frac{\text{BE}}{Mc^2} \simeq \frac{11}{21}\beta + \frac{7187}{18018}\beta^2 + \dots$$

$$P, c_s^2 < \infty \implies \phi_c < \pi/2 \implies \beta < 0.3862, \quad c_s^2 < 1 \implies \beta < 0.2698.$$

Buchdahl's Solution: Relativistic n=1 Polytrope

$$\varepsilon = \sqrt{P_* P} - 5P$$

$$\begin{aligned}
e^{\nu(r)} &= (1 - 2\beta)(1 - \beta - u(r))(1 - \beta + u(r))^{-1}, \\
e^{\lambda(r)} &= (1 - 2\beta)(1 - \beta + u(r))(1 - \beta - u(r))^{-1}(1 - \beta + \beta \cos Ar')^{-2}, \\
8\pi P(r) &= A^2 u(r)^2 (1 - 2\beta)(1 - \beta + u(r))^{-2}, \\
8\pi \varepsilon(r) &= 2A^2 u(r)(1 - 2\beta)(1 - \beta - 3u(r)/2)(1 - \beta + u(r))^{-2}, \\
n(r)m_b c^2 &= \sqrt{p_* p(r)} \left(1 - 4\sqrt{\frac{p(r)}{p_*}} \right)^{3/2}, \quad c_s^2(r) = \left(\frac{1}{2}\sqrt{\frac{p_*}{p(r)}} - 5 \right)^{-1} \\
u(r) &= \frac{\beta}{Ar'} \sin Ar' = (1 - \beta) \left(\frac{1}{2}\sqrt{\frac{P_*}{P(r)}} - 1 \right)^{-1}, \\
r' &= r(1 - 2\beta)(1 - \beta + u(r))^{-1}, \\
A^2 &= 2\pi P_*(1 - 2\beta)^{-1}, \quad R = (1 - \beta) \sqrt{\frac{\pi c^2}{2GP_*(1 - 2\beta)}}. \\
P_c &= \frac{P_*}{4}\beta^2, \quad \varepsilon_c = \frac{P_*}{2}\beta(1 - \frac{5}{2}\beta), \quad n_c m_b c^2 = \frac{P_*}{2}\beta(1 - 2\beta)^{3/2} \\
\text{BE}/(Mc^2) &= (1 - 3/2\beta)(1 - 2\beta)^{-1/2}(1 - \beta)^{-1} \simeq \beta/2 + \beta^2/2 + \dots \\
c_s^2 < \infty &\implies \beta < 1/5, \quad c_s^2 < 1 \implies \beta < 1/6.
\end{aligned}$$

Tolman IV Variation: A Self-Bound Star (Quark Star)

$$e^{\nu(r)} = \frac{[1 - \beta (\frac{5}{2} - \frac{1}{2}x)]^2}{(1 - 2\beta)},$$

$$e^{\lambda(r)} = \frac{[1 - \beta (\frac{5}{2} - \frac{3}{5}x)]^{2/3}}{[1 - \beta (\frac{5}{2} - \frac{3}{2}x)]^{2/3} - 2(1 - \beta)^{2/3}\beta x},$$

$$4\pi \frac{G}{c^2} p R^2 = \frac{\beta}{1 - \beta (\frac{5}{2} - \frac{1}{2}x)} \left[1 - (1 - \beta)^{2/3} \frac{1 - \frac{5}{2}\beta(1 - x)}{[1 - \beta (\frac{5}{2} - \frac{3}{2}x)]^{2/3}} \right],$$

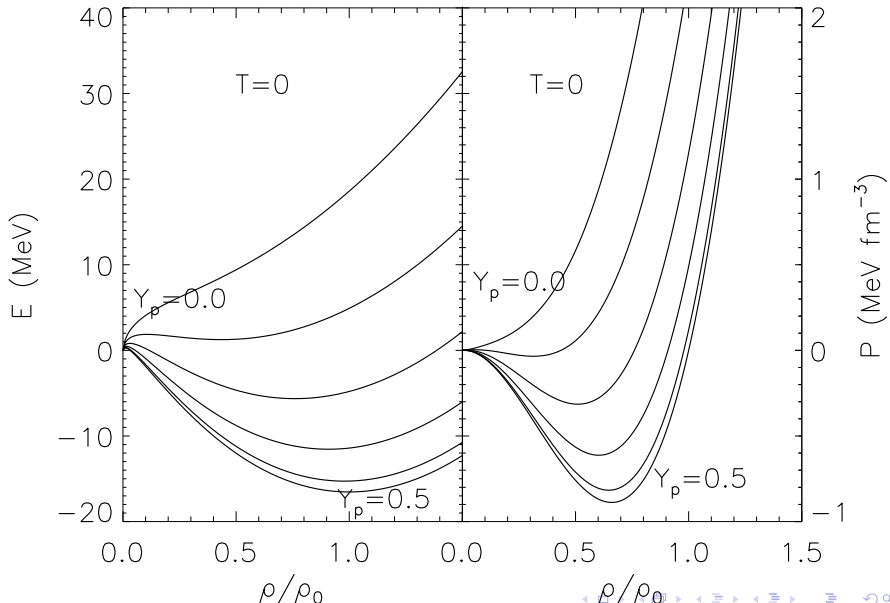
$$4\pi \frac{G}{c^2} \varepsilon R^2 = \frac{3(1 - \beta)^{2/3} \beta [1 - \beta (\frac{5}{2} - \frac{5}{6}x)]}{[1 - \beta (\frac{5}{2} - \frac{3}{2}x)]^{5/3}}, \quad m = \frac{(1 - \beta)^{2/3} M x^{3/2}}{[1 - \beta (\frac{5}{2} - \frac{3}{2}x)]^{2/3}}$$

$$c_s^2 = \frac{(2 - 5\beta + 3\beta x)}{5(2 - 5\beta + \beta x)^3} \left[\frac{(2 - 5\beta + 3\beta x)^{5/3}}{2^{2/3}(1 - \beta)^{2/3}} + (2 - 5\beta)^2 - 5\beta^2 x \right],$$

$$\frac{\varepsilon_{surf}}{\varepsilon_c} = \left(1 - \frac{5}{3}\beta\right) \left(1 - \frac{5}{2}\beta\right)^{2/3} (1 - \beta)^{-5/3}.$$

$$0.30 < c_{s,c}^2 < 0.44, \quad 0.265 < \frac{\varepsilon_{surf}}{\varepsilon_c} < 1$$

Bulk Matter Energy and Pressure



Schematic Free Energy Density

$F(n, x, T)$; n : number density; x : proton fraction; T : temperature

$n_s \simeq 0.16 \pm 0.01 \text{ fm}^{-3}$: nuclear saturation density

$B \simeq 16 \pm 1 \text{ MeV}$: saturation binding energy

$K'_s \simeq -200 \pm 200 \text{ MeV}$:
skewness

$K_s \simeq 240 \pm 20 \text{ MeV}$: incompressibility

$J \simeq 30 \pm 6 \text{ MeV}$: bulk symmetry energy

$K_{\text{sym}} \simeq -300 \pm 300 \text{ MeV}$:
symmetry incompressibility

$L \simeq 60 \pm 60 \text{ MeV}$: symmetry stiffness

$a \simeq 0.065 \pm 0.010 \text{ MeV}^{-1}$: bulk level density parameter

$$F = n \left[-B + \frac{K}{18} \left(1 - \frac{n}{n_s} \right)^2 + J \frac{n}{n_s} (1 - 2x)^2 - a \left(\frac{n_s}{n} \right)^{2/3} T^2 \right]$$

$$P = n^2 \frac{\partial(F/n)}{\partial n} = \frac{n^2}{n_s} \left[\frac{K}{9} \left(\frac{n}{n_s} - 1 \right) + J(1 - 2x)^2 \right] + \frac{2an}{3} \left(\frac{n_s}{n} \right)^{2/3} T^2$$

$$\begin{aligned} \mu_n &= \frac{\partial F}{\partial n} - \frac{x \partial F}{n \partial x} \\ &= -B + \frac{K}{18} \left(1 - \frac{n}{n_s} \right) \left(1 - 3 \frac{n}{n_s} \right) + 2J \frac{n}{n_s} (1 - 2x) - \frac{a}{3} \left(\frac{n_s}{n} \right)^{2/3} T^2 \end{aligned}$$

$$\hat{\mu} = -\frac{1}{n} \frac{\partial F}{\partial x} = \mu_n - \mu_p = 4J \frac{n}{n_s} (1 - 2x)$$

$$s = -\frac{1}{n} \frac{\partial F}{\partial T} = 2a \left(\frac{n_s}{n} \right)^{2/3} T; \quad \varepsilon = F + nTs$$

Nuclear Symmetry Energy

Defined as the difference between energies of pure neutron matter ($x = 0$) and symmetric ($x = 1/2$) nuclear matter.

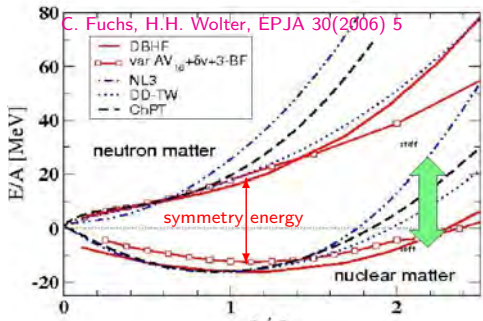
$$S(\rho) = E(\rho, x = 0) - E(\rho, x = 1/2)$$

Expanding around saturation density (ρ_s) and symmetric matter ($x = 1/2$)

$$E(\rho, x) = E(\rho, 1/2) + (1-2x)^2 S_2(\rho) + \dots$$

$$S_2(\rho) = J + \frac{L}{3} \frac{\rho - \rho_s}{\rho_s} + \dots$$

$$J \simeq 31 \text{ MeV}, L \simeq 50 \text{ MeV}$$



Connections to neutron matter:

$$E(\rho_s, 0) \approx J + E(\rho_s, 1/2) = J - B, \quad P(\rho_s, 0) = L\rho_s/3$$

Neutron star matter (in beta equilibrium):

$$\frac{\partial(E + E_e)}{\partial x} = 0, \quad P(\rho_s, x_\beta) \simeq \frac{L\rho_s}{3} \left[1 - \left(\frac{4J}{\hbar c} \right)^3 \frac{4 - 3J/L}{3\pi^2 \rho_s} \right]$$

The Liquid Drop Model of Nuclei

$$E(Z, N) \simeq -BA + JAI^2 + (E_s - S_s I^2)A^{2/3} + E_C \frac{Z^2}{A^{1/3}}$$

$B \simeq 16$ MeV, $J \simeq 30$ MeV, $E_s \simeq 18$ MeV, $S_s \simeq 45$ MeV, $E_C \simeq 0.75$ MeV.

At each density, the preferred nucleus has a mass determined by

$$\left(\frac{\partial(E/A)}{\partial A} \right)_x = -\frac{E_s - S_s I^2}{3A^{4/3}} + \frac{2E_C x^2}{3A^{1/3}} = 0$$

. The Nuclear Virial Theorem is surface energy is twice Coulomb energy:

$$E_s - S_s I^2 = 2E_C x^2 A, \quad A_{opt} = 2 \frac{E_s - S_s I^2}{E_C (1 - I)^2} \simeq 48(1 + 2I) \simeq 61.$$

At low densities (neglect electrons), the optimum proton fraction is

$$\left(\frac{\partial(E/A)}{\partial x} \right)_A = -4I \left(J - \frac{S_s}{A^{1/3}} \right) + (1 - I)E_C A^{2/3} = 0,$$

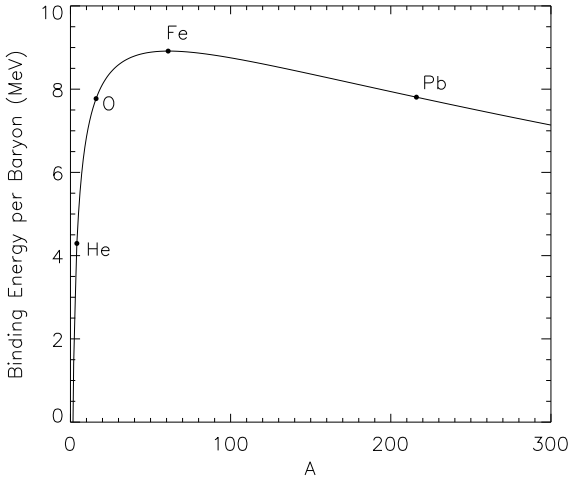
$$I = \frac{E_C A}{4(JA^{1/3} - S_s) + E_C A} \simeq 0.125; \quad Z \simeq 27$$

S_s is nearly linearly correlated with the symmetry parameter L , as it reflects energy contributions from having extra neutrons near the surface.

Isolated Nuclei

The binding energy curve is heavily skewed. Certain closed-shell nuclei (He, C, O, Pb) have much larger binding than the average.

The optimum value of I increases with mass number A . This trend represents the *Valley of Beta Stability*.



Nuclear Droplet Model

Myers & Swiatecki droplet extension: consider the variation of the neutron/proton asymmetry within the nuclear surface.

$$E(A, Z) = (-B + J\delta^2)(A - N_s) + (E_s - S_s\delta^2)A^{2/3} + E_C Z^2 A^{-1/3} + \mu_n N_s.$$

N_s is the number of excess neutrons associated with the surface,

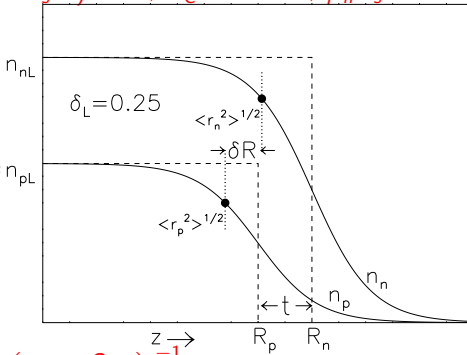
$$\delta = 1 - 2x = (A - N_s - 2Z)/(A - N_s)$$

is the asymmetry of the nuclear bulk fluid, and $\mu_n = -a_v + J\delta(2 - \delta)$ is the neutron chemical potential. Surface tension is the surface thermodynamic potential; adding $\mu_n N_s$ gives the total surface energy. Optimizing $E(A, Z)$ with respect to N_s yields

$$N_s = \frac{S_s}{J} \frac{\delta}{1 - \delta} = A \frac{1 - \delta}{1 - \delta}, \quad \delta = I \left(1 + \frac{S_s}{JA^{1/3}} \right)^{-1},$$

$$E(A, Z) = -BA + E_s A^{2/3} + E_C Z^2 / A^{1/3} + JAI^2 \left(1 + \frac{S_s}{JA^{1/3}} \right)^{-1}.$$

Note that neutron skin thickness depends on $S_s/J \propto L$.



Symmetry Parameters are Highly Correlated

Assuming approximate validity of liquid drop model:

$$E_{\text{sym}}(N, Z) = (JA - S_s A^{2/3})/I^2$$

$$\chi^2 = \frac{1}{N\sigma_D^2} \sum_{i=1}^N (E_{\text{ex},i} - E_{\text{sym},i})^2$$

$$\chi_{vv} = \frac{2}{N\sigma_D^2} \sum_{i=1}^N I_i^4 A_i^2 = 61.6 \sigma_D^{-2}$$

$$\chi_{vs} = -\frac{2}{N\sigma_D^2} \sum_{i=1}^N I_i^4 A_i^{5/3} = -10.7 \sigma_D^{-2}$$

$$\chi_{ss} = \frac{2}{N\sigma_D^2} \sum_{i=1}^N I_i^4 A_i^{4/3} = 1.87 \sigma_D^{-2}$$

$$\sigma_J = \sqrt{\frac{2\chi_{ss}}{\chi_{vv}\chi_{ss} - \chi_{sv}^2}} \approx 2.3 \sigma_D$$

$$\sigma_{S_s} = \sqrt{\frac{2\chi_{vv}}{\chi_{vv}\chi_{ss} - \chi_{sv}^2}} \approx 13.2 \sigma_D$$

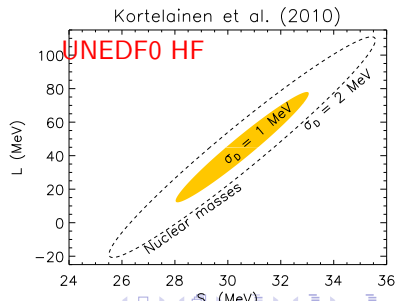
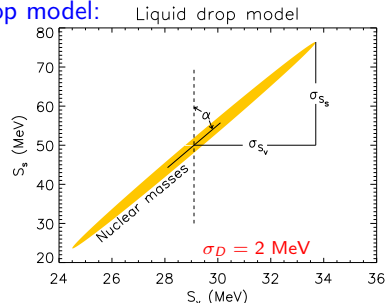
$$\alpha = \frac{1}{2} \tan^{-1} \frac{2\chi_{vs}}{\chi_{vv} - \chi_{ss}} \approx 9^\circ.8$$

$$r_{vs} = -\frac{\chi_{vs}}{\sqrt{\chi_{vv}\chi_{ss}}} \approx 0.997$$

Liquid droplet model:

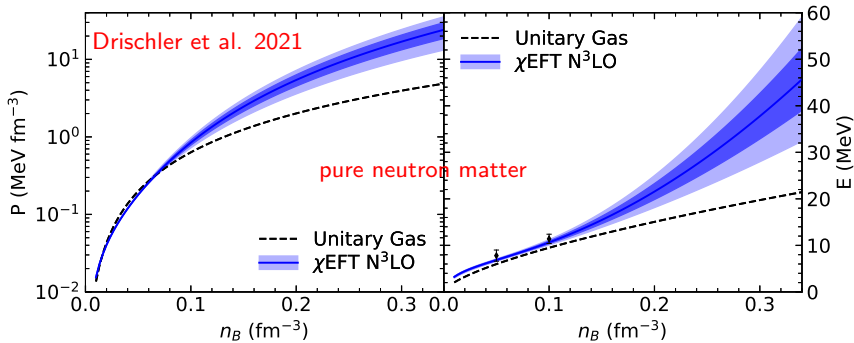
$$E_{\text{sym}}(N, Z) = \frac{JAI^2}{1 + (S_s/J)A^{-1/3}}$$

$$S_s \simeq \frac{3a}{2r_o} S_v [1 + (L/3J) + (L/3J)^2 + \dots]$$



Theoretical Neutron Matter Studies

Recently developed chiral effective field theory allows a systematic expansion of nuclear forces at low energies based on the symmetries of quantum chromodynamics. It exploits the gap between the pion mass (the pseudo-Goldstone boson of chiral symmetry-breaking) and the energy scale of short-range nuclear interactions established from experimental phase shifts. It provides the only known consistent framework for estimating energy uncertainties.



Symmetry Parameters From Neutron Matter

Pure neutron matter calculations are more reliable than symmetric matter calculations.

Symmetric matter has delicate cancellations sensitive to short- and intermediate-range three-body interactions at N²LO that are Pauli-blocked in neutron matter.

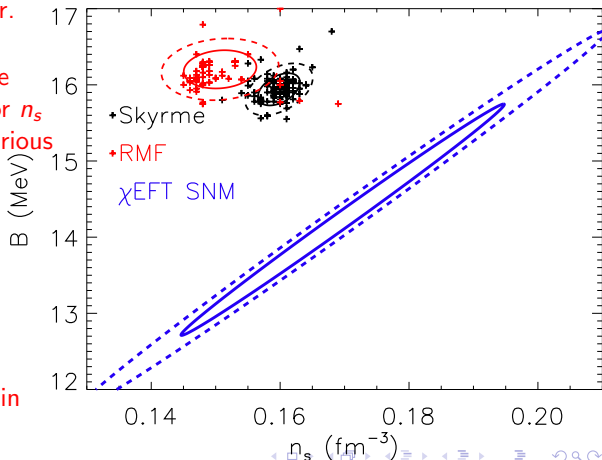
N³LO symmetric matter calculations don't saturate within empirical ranges for n_s and B , and introduce spurious correlations in symmetric matter.

Instead, infer symmetry parameters from

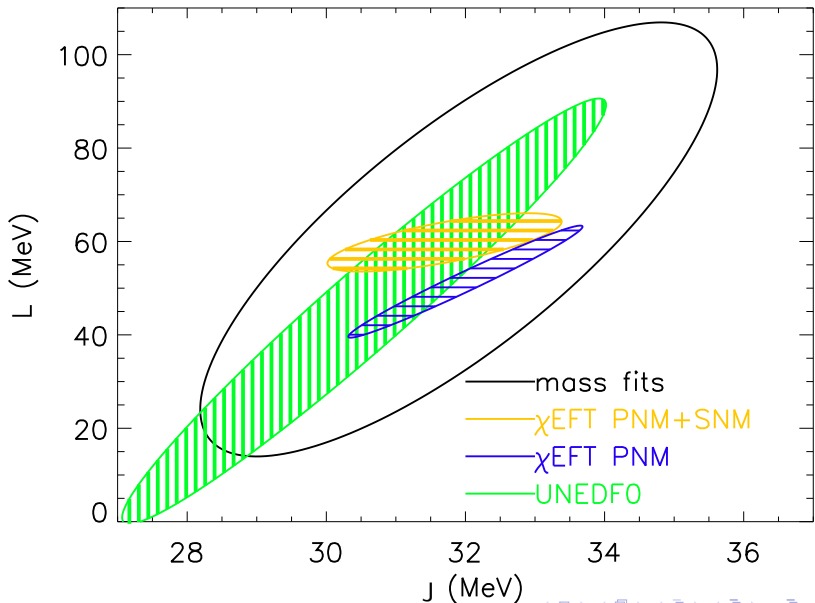
$$J = E_N(n_s) + B$$

$$L = 3P_N(n_s)/n_s$$

and include uncertainties in E_N , P_N , n_s and B .



Correlations From Chiral EFT



Bounds From The Unitary Gas Conjecture

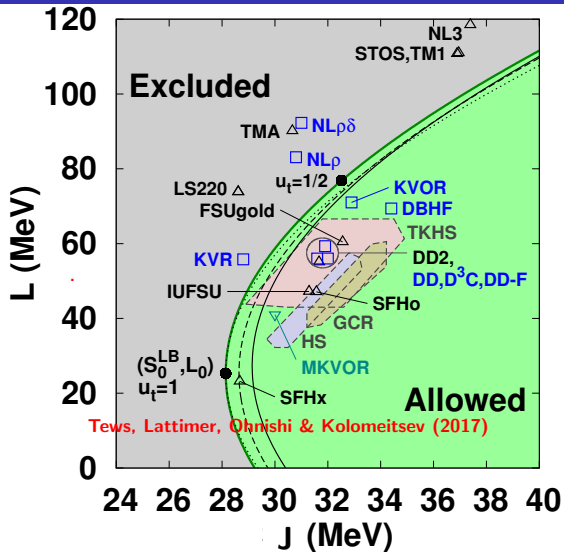
The Conjecture (UGC):

Neutron matter energy always larger than unitary gas energy.

$$E_{UG} = \xi_0(3/5)E_F, \text{ or}$$

$$E_{UG} \simeq 12.6 \left(\frac{n}{n_s} \right)^{2/3} \text{ MeV.}$$

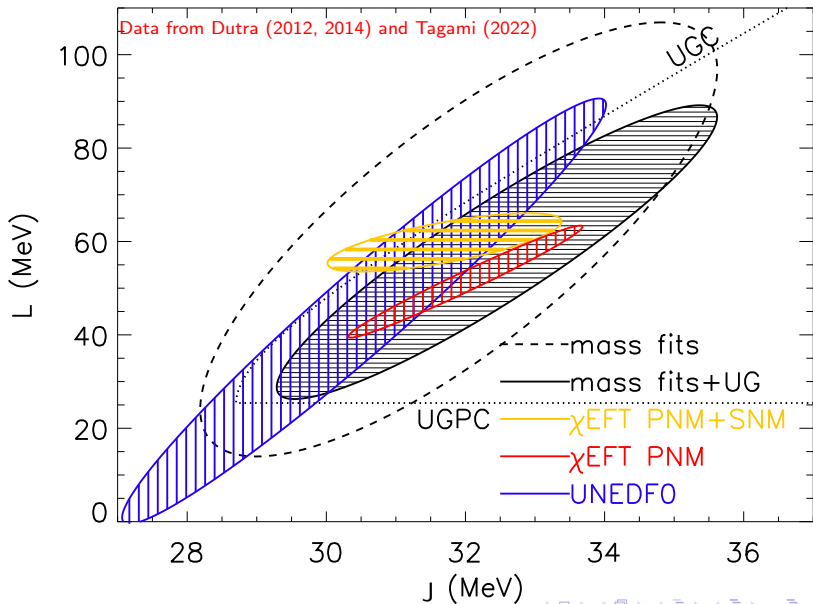
The unitary gas consists of fermions interacting via a pairwise short-range s-wave interaction with infinite scattering length and zero range. Cold atom experiments show a universal behavior with the Bertsch parameter $\xi_0 \simeq 0.37$.



For $n \geq n_s$, one also observes $P_N > P_{UG}$ (UGPC).

$J \geq 28.6$ MeV; $L \geq 25.3$ MeV; $P_N(n_s) \geq 1.35$ MeV fm⁻³; $R_{1.4} \geq 9.7$ km

Applying Unitary Gas Constraints

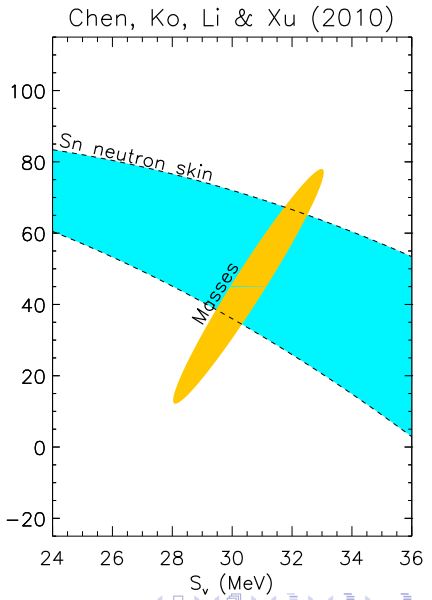
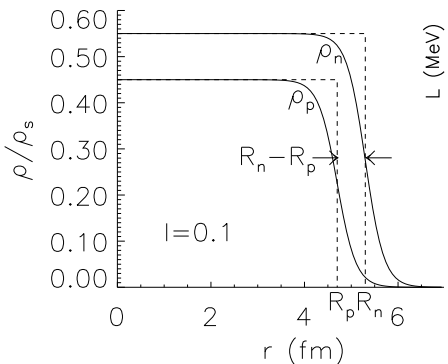


Nuclear Experimental Constraints

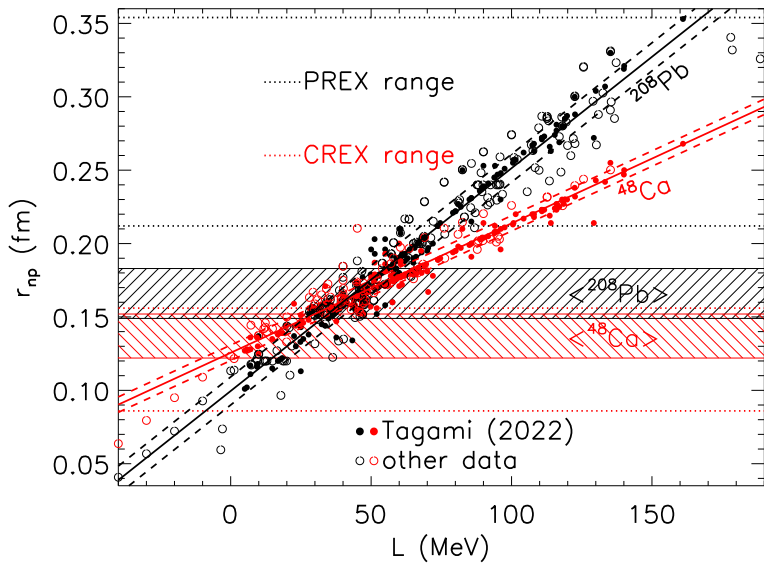
Neutron Skin Thicknesses

$$r_{np} = \frac{2r_o}{3J} \frac{1}{\sqrt{1-l^2}} (1 + S_s A^{-1/3} / J)^{-1}$$
$$\times \sqrt{\frac{3}{5}} \left[IS_s - \frac{3Ze^2}{140r_o} \left(1 + \frac{10}{3} \frac{S_s A^{-1/3}}{J} \right) \right]$$

$$r_{np,208} = 0.15 \pm 0.04 \text{ fm}$$



Calculated $L - r_{np}$ Correlations



Implied L Values

Historical experimental weighted average ^{208}Pb
 $r_{np}^{208} = 0.166 \pm 0.017 \text{ fm}$, implying $L = 45 \pm 13 \text{ MeV}$.

Historical experimental weighted average ^{48}Ca
 $r_{np}^{48} = 0.137 \pm 0.015 \text{ fm}$, implying $L = 14 \pm 21 \text{ MeV}$.

Combined $L = 36 \pm 11 \text{ MeV}$.

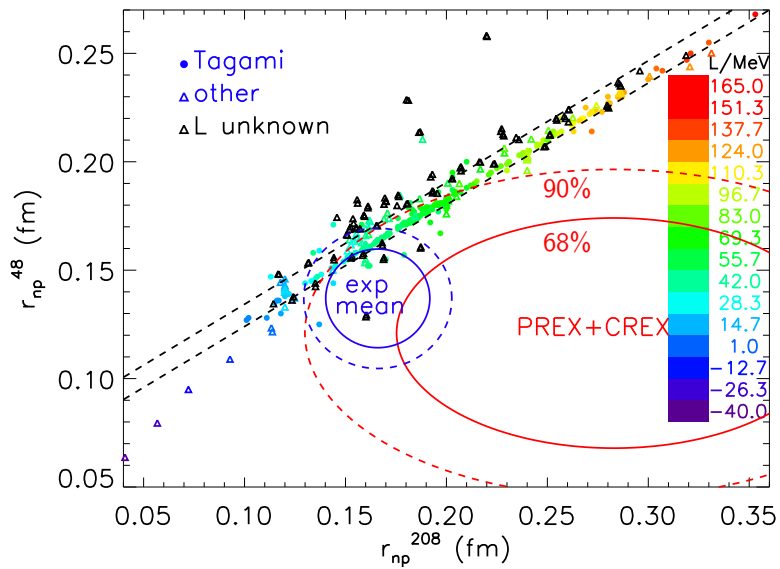
Parity-violating electron scattering measurements at JLab:

PREX I+II ^{208}Pb (Adhikari et al. 2021):
 $r_{np}^{208} = 0.283 \pm 0.071 \text{ fm}$, implying $L = 119 \pm 46 \text{ MeV}$.

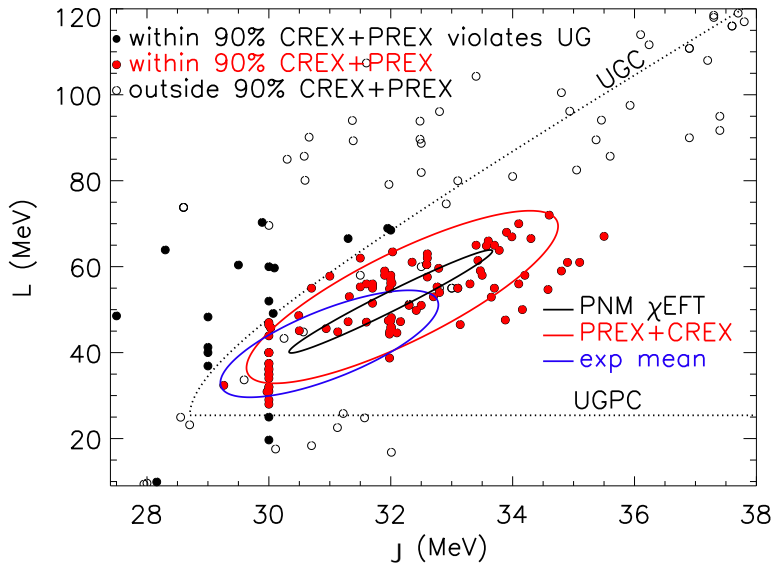
CREX ^{48}Ca (Adhikari et al. 2022):
 $r_{np}^{48} = 0.121 \pm 0.035 \text{ fm}$, implying $L = -5 \pm 42 \text{ MeV}$.

Combined $L = 51 \pm 31 \text{ MeV}$.

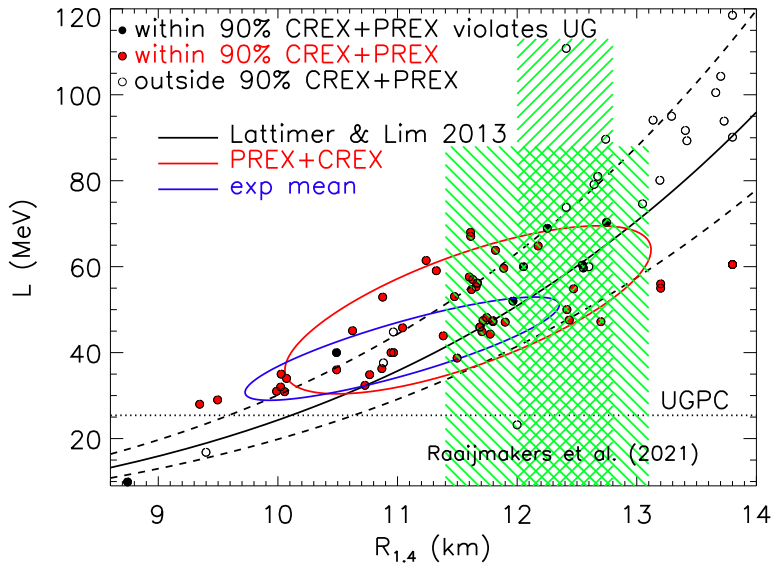
$r_{np}^{208} - r_{np}^{48}$ Linear Correlation



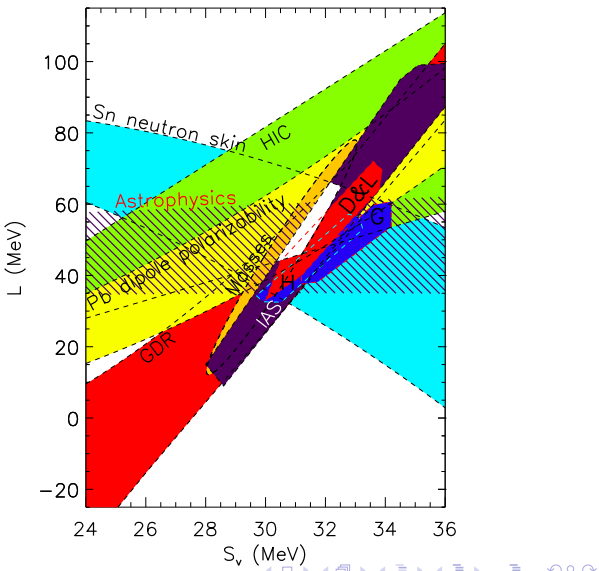
Implied $J - L$



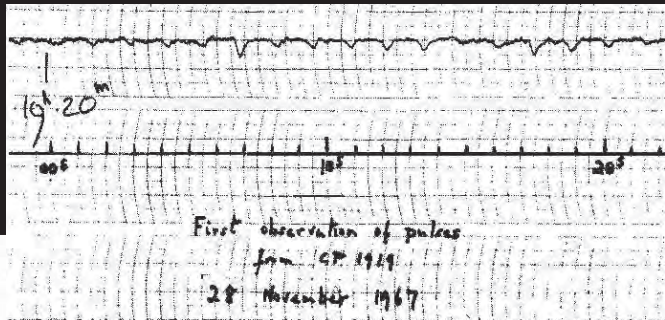
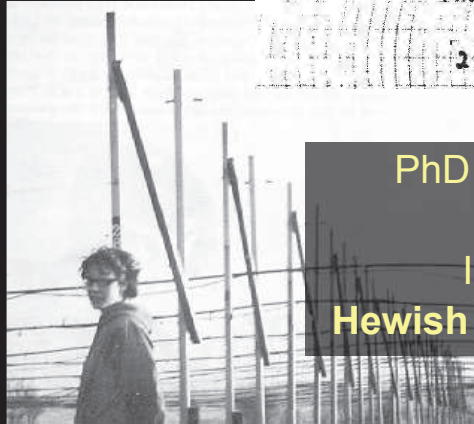
Implied $R_{1.4} - L$



Combined Constraints



The Discovery of Pulsars



PhD student **Jocelyn Bell** and
Prof. **Antony Hewish**
Initially “Little Green Men”
Hewish won Nobel Prize in 1974

Crab Nebula SN1054AD



Anasazi Indian cave pictogram,
Chaco Canyon, NM

J. M. Lattimer

Neutron Star Structure and Measurements

O

Pulsar rotates
30 times
per second!

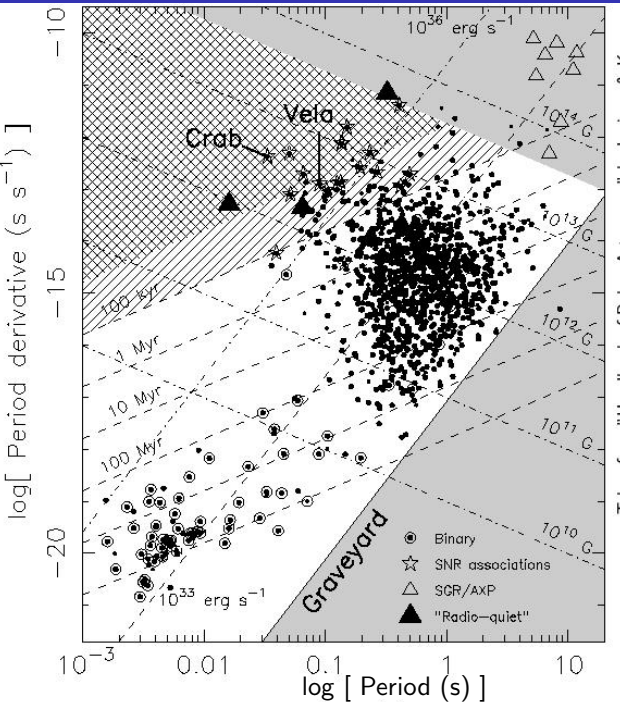
$P - \dot{P}$ Diagram

$$\tau_c = \frac{P}{2\dot{P}}$$

$$B \simeq 3 \cdot 10^{19} \sqrt{P \dot{P}} \text{ G}$$

$$-\dot{E} \simeq 10^{47} \frac{\dot{P}}{P^3} \text{ erg/s}$$

P in seconds

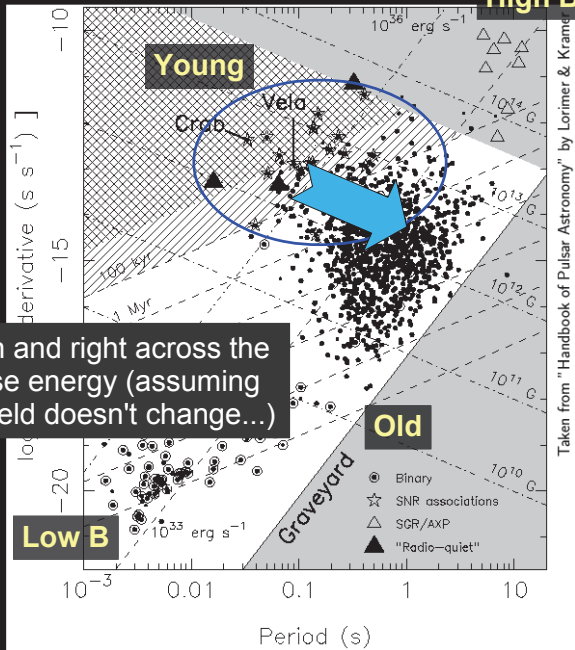


Taken from "Handbook of Pulsar Astronomy" by Lorimer & Kramer

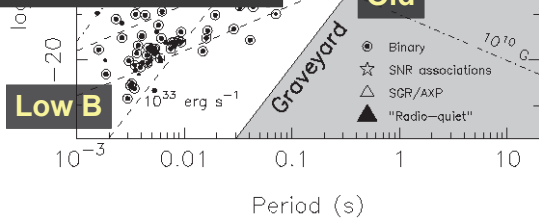
Pulsar Flavors

Young PSRs

(high B, fast spin,
very energetic)



Pulsars move down and right across the diagram as they lose energy (assuming that the magnetic field doesn't change...)



Pulsar Flavors

Young PSRs

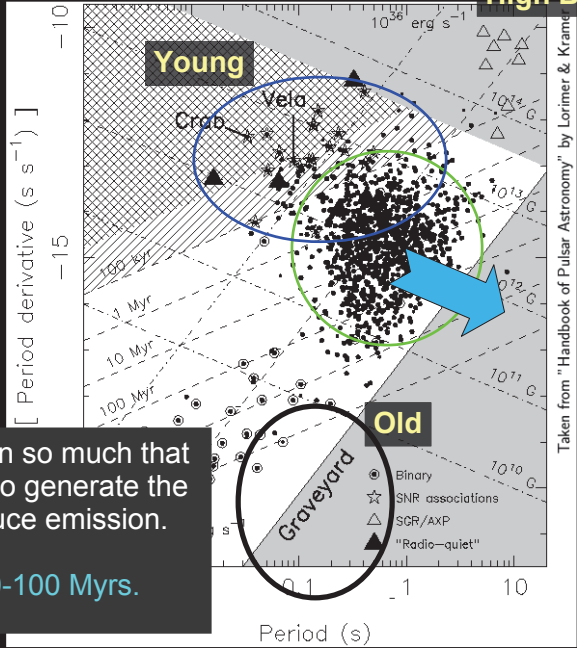
(high B, fast spin,
very energetic)

Normal PSRs

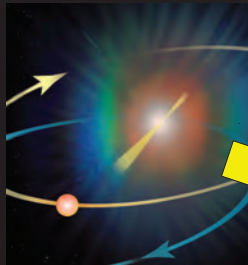
(average B,
slow spin)

Eventually they slow down so much that there is not enough spin to generate the electric fields which produce emission.

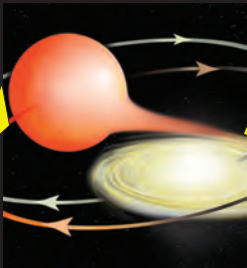
Their lifetimes are 10-100 Myrs.



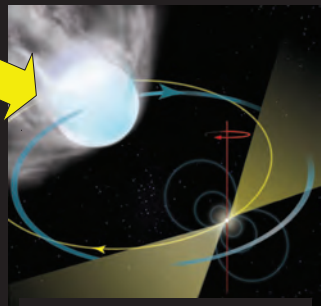
Millisecond Pulsars: via “Recycling”



Supernova produces
a neutron star



Red Giant transfers
matter to neutron star



Millisecond Pulsar
emerges with a white
dwarf companion

Alpar et al 1982
Radhakrishnan & Srinivasan 1984

Picture credits: Bill Saxton, NRAO/AUI/NSF

Pulsar Flavors

Young PSRs

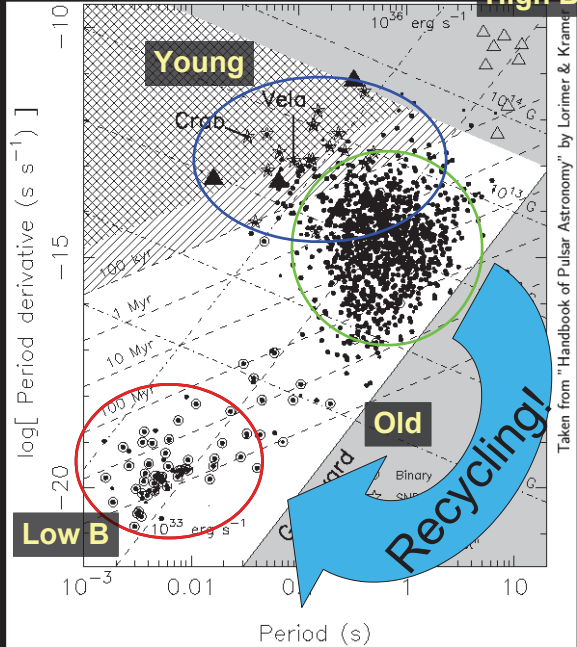
(high B, fast spin,
very energetic)

Normal PSRs

(average B,
slow spin)

Millisecond PSRs

(low B, very fast,
very old, very stable
spin, best for basic
physics tests)



Taken from "Handbook of Pulsar Astronomy" by Lorimer & Kramer

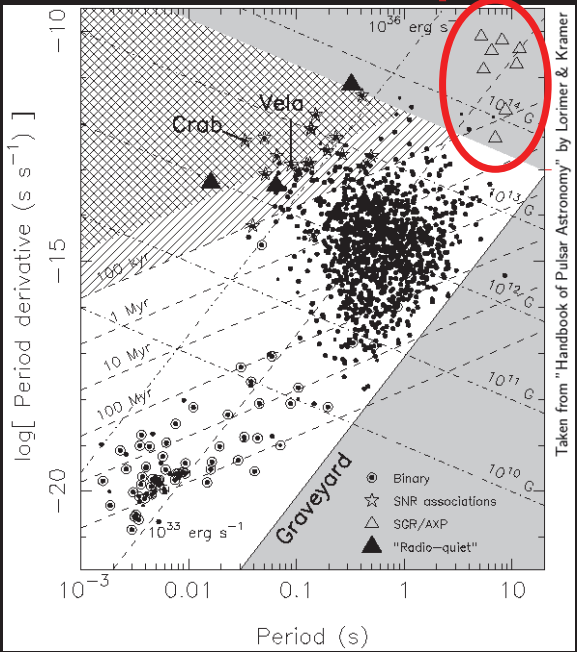
What's a Magnetar?

Neutron stars with **extremely strong** magnetic fields:

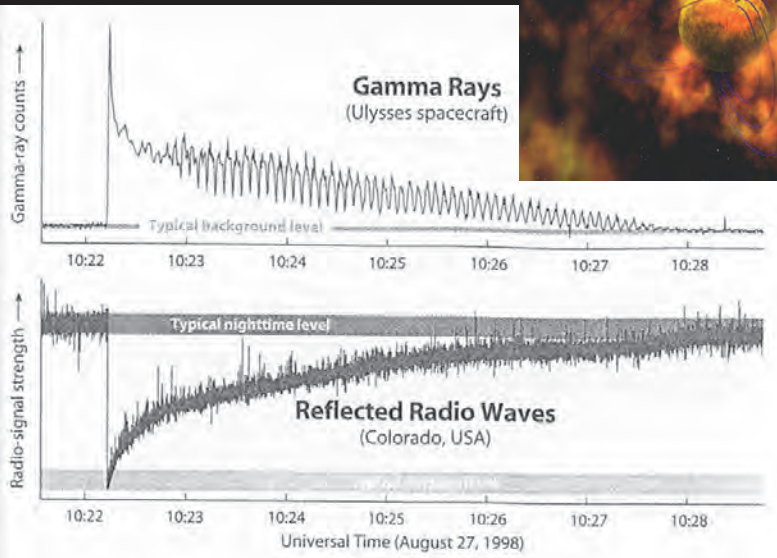
10^{14-15} Gauss

(~1000x stronger than normal PSRs)

Powered by decay of magnetic field, not rotation!



Giant X-ray Flares: Magnetar SGR 1900+14



Pulsars are Precise Clocks

PSR J0437-4715

At 00:00 UT Jan 18 2011:

$$P = 5.7574519420243 \text{ ms}$$
$$+/- 0.0000000000001 \text{ ms}$$

The last digit changes by 1 every half hour!

This digit changes by 1 every 500 years!

This extreme precision is what allows us to
use pulsars as tools to do unique physics!

Pulsar Timing:

Pulse Phase Tracking

Unambiguously account for every rotation of a pulsar over years

Measurement
(TOAs: Times of Arrival)

Observation 1



Pulses



Obs 2

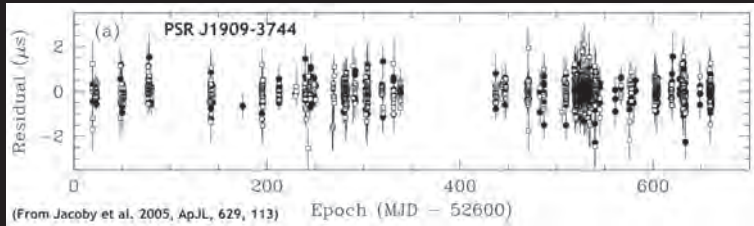


Model
(prediction)

Obs 3

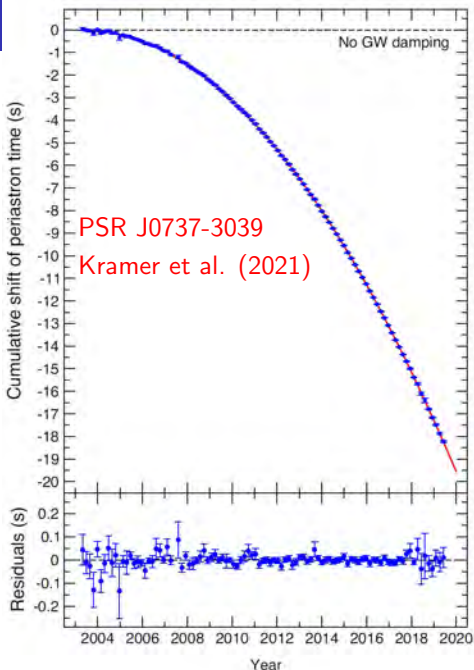


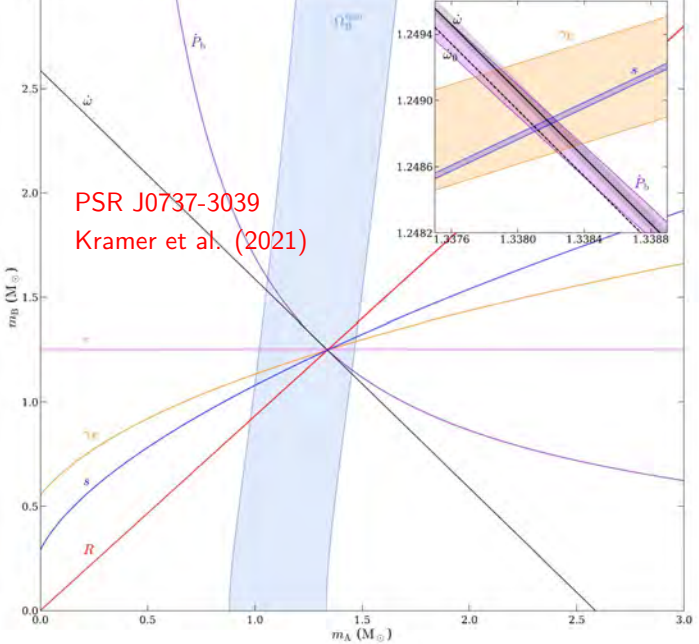
Measurement - Model = Timing Residuals



200ns RMS
over 2 yrs

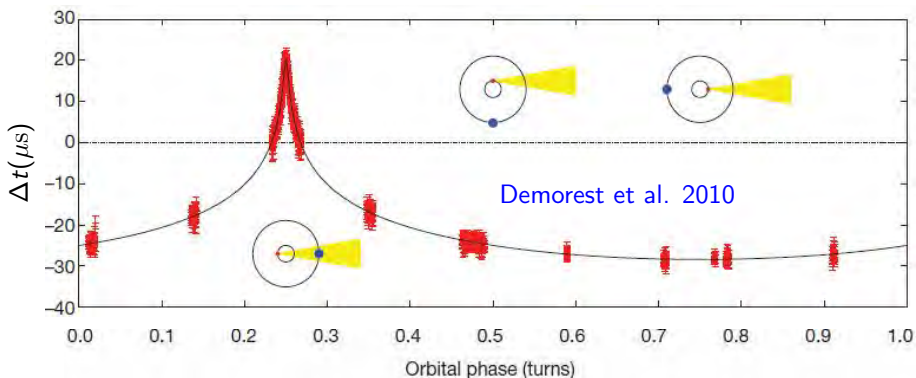
PSR J0737-3039





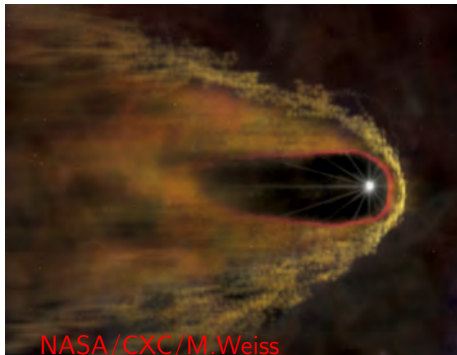
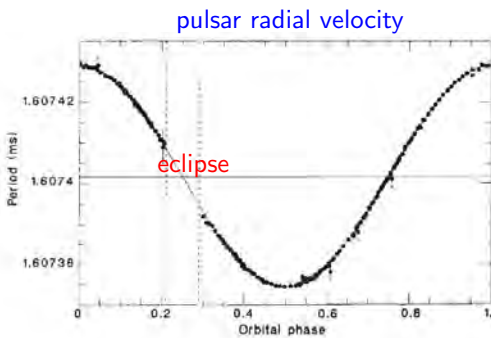
PSR J1614-2230

3.15 ms pulsar in 8.69d orbit with $0.5 M_{\odot}$ white dwarf companion.
Shapiro delay tightly confines the edge-on inclination: $\sin i = 0.99984$
Pulsar mass is $1.97 \pm 0.04 M_{\odot}$
Distance > 1 kpc, $B \simeq 1.8 \times 10^8$ G

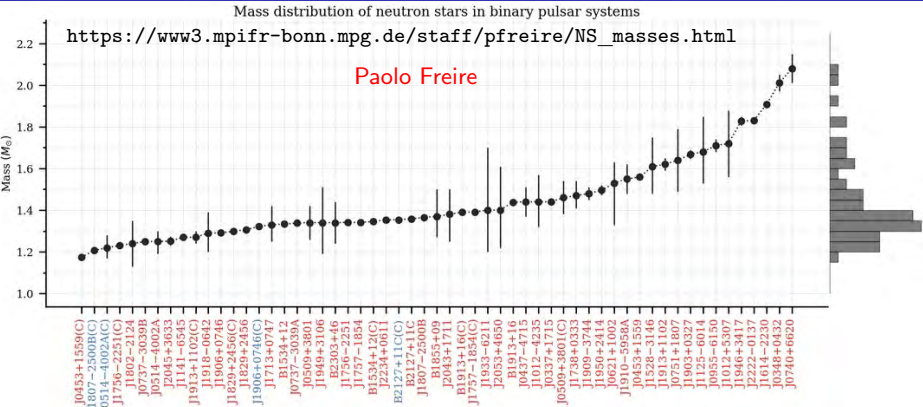


Black Widow Pulsar PSR B1957+20

A 1.6ms pulsar in circular 9.17h orbit with $\sim 0.03 M_{\odot}$ companion. The pulsar is eclipsed for 50-60 minutes each orbit; the eclipsing object has a volume much larger than the secondary or its Roche lobe. The pulsar is ablating the companion leading to mass loss and the eclipsing plasma cloud. The secondary may nearly fill its Roche lobe. Ablation by the pulsar leads to secondary's eventual disappearance. The optical light curve tracks the motion of the secondary's irradiated hot spot rather than its center of mass motion.



Masses of Pulsars in Binaries from Pulsar Timing



Largest: $2.08 \pm 0.07 M_{\odot}$

Smallest: $1.174 \pm 0.004 M_{\odot}$

Several other NS masses have been measured by other means, including some estimated to be more than $2M_{\odot}$ (e.g., black widow pulsars) and smaller than $1M_{\odot}$ (HESS J1731-347), but their mass uncertainties are generally large.

What is the Maximum Mass?

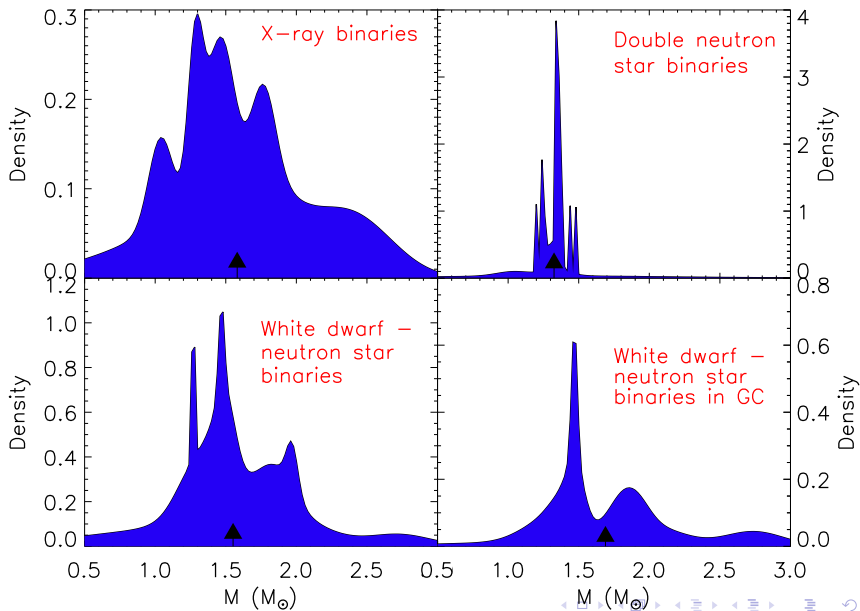
Pulsar mass measurements, giving lower limits to M_{\max}

- ▶ PSR J1614+2230 (Demorest et al. 2010) $M = 1.97 \pm 0.04 M_{\odot}$; a nearly edge-on system with well-measured Shapiro time delay.
- ▶ PSR J0548+0432 (Antoniadis et al. 2013) $M = 2.01 \pm 0.04 M_{\odot}$; measured using optical data and theoretical properties of companion white dwarf.
- ▶ B1957+20 (van Kerkwijk 2010) $M = 2.4 \pm 0.3 M_{\odot}$; black widow pulsar (BWP).
- ▶ PSR J1311-3430 (Romani et al. 2012) $M = 2.55 \pm 0.50 M_{\odot}$; BWP.
- ▶ PSR J1544+4937 (Tang et al. 2014) $M = 2.06 \pm 0.56 M_{\odot}$; BWP.
- ▶ PSR 2FGL J1653.6-0159 (Romani et al. 2014)
 $M > f(M_2)/\sin^3 i \gtrsim 1.96 M_{\odot}$; largest $f(M_2)$.
- ▶ PSR J1227-4859 (de Martino et al. 2014) $M = 2.2 \pm 0.8 M_{\odot}$; redback pulsar.
- ▶ PSR J0952-0607 (Romani et al. 2022) $M = 2.35 \pm 0.17 M_{\odot}$; BWP.

Theoretical upper limit to M_{\max}

- ▶ GW170817 $M_{\max} \leq 2.2 - 2.3 M_{\odot}$.

The Distribution of Neutron Star Masses



How Can a Neutron Star's Radius Be Measured?

- Flux = $\frac{\text{Luminosity}}{4\pi D^2} = \frac{4\pi R^2 \sigma_B T_s^4}{4\pi D^2} = \left(\frac{R}{D}\right)^2 \sigma_B T_s^4$
X-ray observations of quiescent neutron stars in low-mass X-ray binaries measure the flux and surface temperature T_s . Distance D somewhat uncertain; GR effects introduce an M dependence.
- $F_{Edd} = \frac{GMc}{\kappa D^2}$ X-ray observations of bursting neutron stars in accreting systems measure the Eddington flux F_{Edd} . κ is the poorly-known opacity; GR effects introduce an R dependence.
- X-ray phase-resolved spectroscopy of millisecond pulsars with nonuniform surface emissions (hot spots). NICER: PSR J0030+0451, PSR J0437-4715 (closest and brightest millisecond pulsar) and PSR J0740+6620 (most massive pulsar).
- $R_{1.4} \simeq (11.5 \pm 0.3) \frac{\mathcal{M}}{M_\odot} \left(\frac{\tilde{\Lambda}}{800}\right)^{1/6} \text{km}, \quad \mathcal{M} = \frac{(M_A M_B)^{3/5}}{(M_A + M_B)^{1/5}}$
GW observations of neutron star mergers measure the chirp mass \mathcal{M} and binary tidal deformability $\tilde{\Lambda}$ (GW170817).
- $I_A \propto M_A R_A^2$ Radio observations of extremely relativistic binary pulsars measure masses M_A, M_B and moment of inertia I_A from spin-orbit coupling [PSR J0737-3039 ($P_b = 0.102$ d), PSR J1757-1854 (0.164 d), PSR J1946+2052 (0.078 d)].

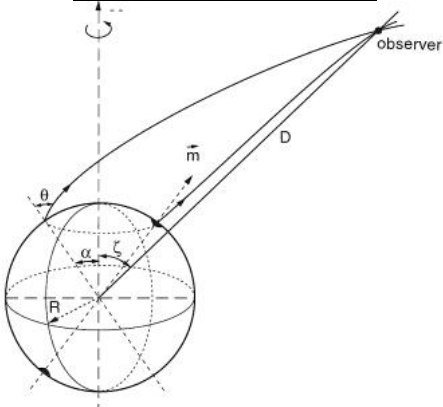
Radiation Radius

- The measurement of flux and temperature yields an apparent angular size (pseudo-BB):

$$\frac{R_\infty}{d} = \frac{R}{d} \frac{1}{\sqrt{1 - 2GM/Rc^2}}$$

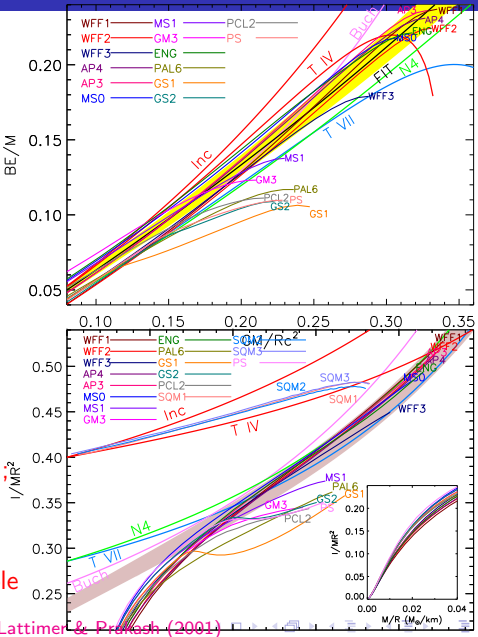
- Observational uncertainties include distance, interstellar H absorption (hard UV and X-rays), atmospheric composition
- Nearby isolated neutron stars (parallax measurable)
- Quiescent X-ray binaries in globular clusters (reliable distances, low B H-atmospheres)
- Bursting sources in which Eddington flux is measured

$$F_{Edd} = \frac{GMc}{\kappa D^2} \sqrt{1 - \frac{2GM}{R_{ph}c^2}}$$



Semi-Universal Relations for Neutron Stars

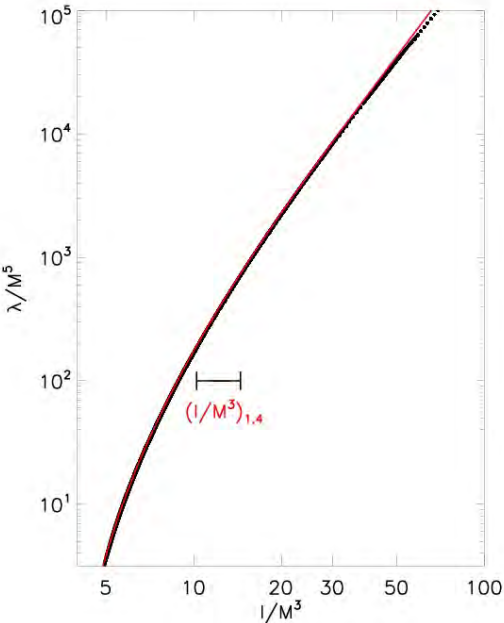
- ▶ The first universal relations discovered for neutron stars connected
 - ▶ pressure and neutron star radius,
 - ▶ binding energy and compactness,
 - ▶ moment of inertia and compactness.
- ▶ Simple explanations exist using analytical TOV solutions that bracket realistic equations of state.
- ▶ Tolman VII: $\varepsilon = \varepsilon_0 [1 - (r/R)^2]$,
- ▶ Buchdahl: $\varepsilon = 12\sqrt{\varepsilon_* p} - 5p$.
- ▶ Easily extended to tidal Love number and rotational quadrupole moment.



I-Love-Q Correlations

Yagi and Yunes (2013) discovered that the moment of inertia I , the tidal love number (tidal response) λ , and the quadrupole polarizability Q are extremely highly correlated.

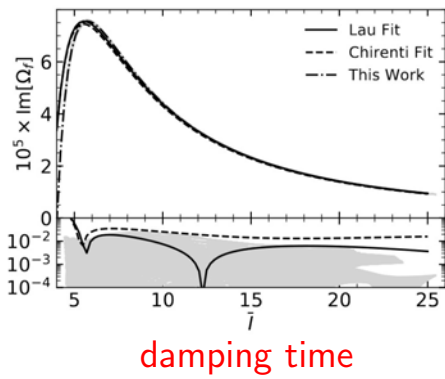
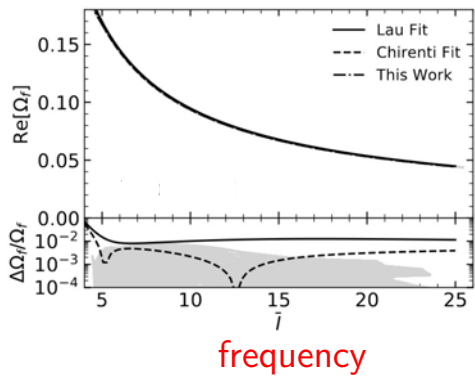
Dimensionless love numbers of neutron stars in a merging binary are, furthermore, universally related, allowing for their individual measurements from gravitational waves of a binary inspiral (Yagi and Yunes 2015).



F-Mode Properties - Moment of Inertia

$$\Omega_f = \frac{GM}{c^3} \omega_f$$

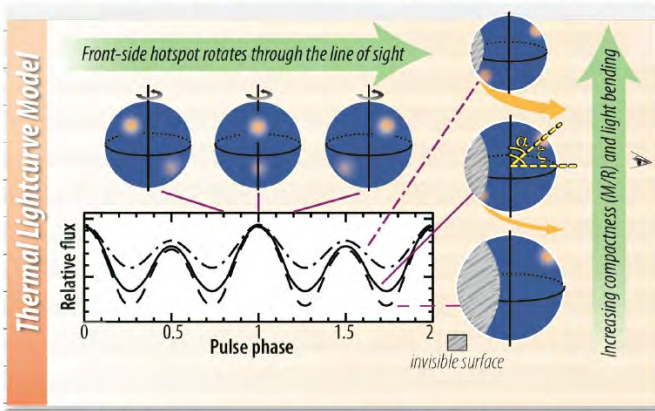
Zhao & Lattimer 2022



Science Measurements

NICER

Reveal stellar structure through lightcurve modeling, long-term timing, and pulsation searches

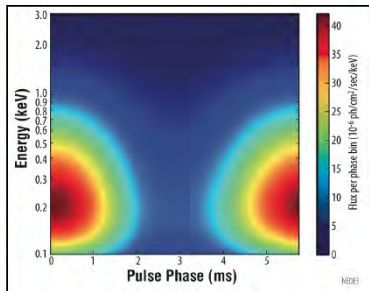


Lightcurve modeling constrains the compactness (M/R) and viewing geometry of a non-accreting millisecond pulsar through the depth of modulation and harmonic content of emission from rotating hot-spots, thanks to gravitational light-bending...

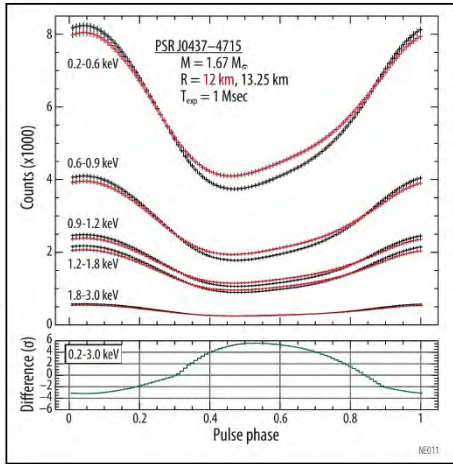


Science Measurements (cont.)

NICER

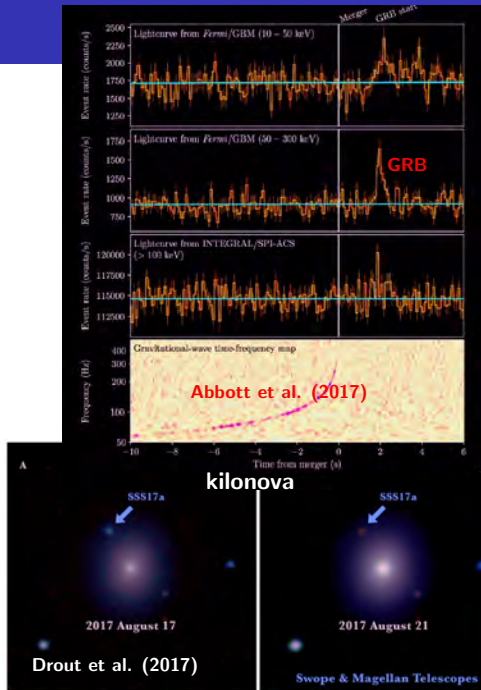


... while phase-resolved spectroscopy promises a direct constraint of radius R .



GW170817

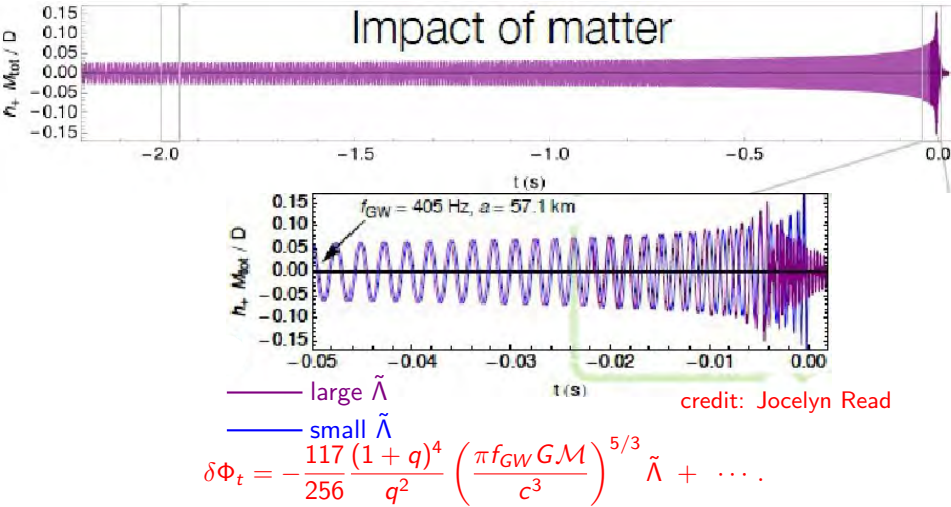
- ▶ LVC detected a signal consistent with a BNS merger, followed 1.7 s later by a weak gamma-ray burst.
- ▶ ≈ 10100 orbits observed over 317 s.
- ▶ $\mathcal{M} = 1.186 \pm 0.001 M_{\odot}$
- ▶ $M_{T,\min} = 2^{6/5} \mathcal{M} = 2.725 M_{\odot}$
- ▶ $E_{\text{GW}} > 0.025 M_{\odot} c^2$
- ▶ $D_L = 40^{+8}_{-14} \text{ Mpc}$
- ▶ $75 < \tilde{\Lambda} < 560$ (90%)
- ▶ $M_{\text{ejecta}} \sim 0.06 \pm 0.02 M_{\odot}$
- ▶ Blue ejected mass: $\sim 0.01 M_{\odot}$
- ▶ Red ejected mass: $\sim 0.05 M_{\odot}$
- ▶ Probable r-process production
- ▶ Ejecta + GRB: $M_{\max} \lesssim 2.22 M_{\odot}$



The Effect of Tides

Tides accelerate the inspiral and produce a gravitational wave phase shift compared to the case of two point masses.

Impact of matter



Tidal Deformability

The tidal deformability λ is the ratio of the induced dipole moment Q_{ij} to the external tidal field E_{ij} , $Q_{ij} \equiv -\lambda E_{ij}$.

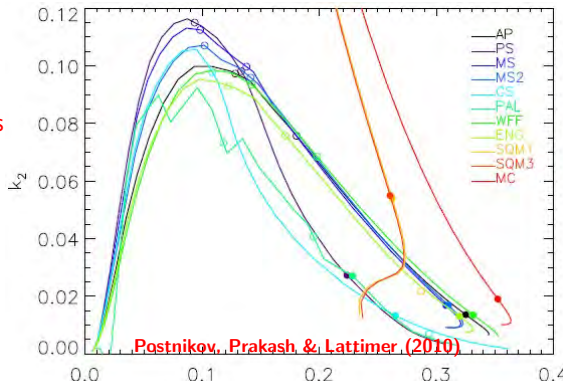
Use $\beta = GM/Rc^2$ and
 $\Lambda = \frac{\lambda c^{10}}{G^4 M^5} \equiv \frac{2}{3} k_2 \beta^{-5}$.

$k_2 \propto 1/\beta$ is the dimensionless Love number, so $\Lambda \simeq a\beta^{-6}$.

For $1 < M/M_\odot < 1.6$,
 $a = 0.0093 \pm 0.0007$.

For a neutron star binary, the mass-weighted $\tilde{\Lambda}$ is the relevant observable:

$$\tilde{\Lambda} = \frac{16}{13} \frac{(1 + 12q)\Lambda_1 + (12 + q)q^4\Lambda_2}{(1 + q)^5},$$



$$\beta = \frac{GM}{Rc^2}$$
$$q = \frac{M_2}{M_1} \leq 1$$

Binary Deformability and the Radius

$$\tilde{\Lambda} = \frac{16}{13} \frac{(1 + 12q)\Lambda_1 + q^4(12 + q)\Lambda_2}{(1 + q)^5} \simeq \frac{16a}{13} \left(\frac{R_{1.4}c^2}{GM} \right)^6 \frac{q^{8/5}(12 - 11q + 12q^2)}{(1 + q)^{26/5}}.$$

This is very insensitive to q for $q > 0.5$, so

$$\tilde{\Lambda} \simeq a' \left(\frac{R_{1.4}c}{GM} \right)^6.$$

For $M = (1.2 \pm 0.2) M_\odot$, $a' = 0.0035 \pm 0.0006$,

$$R_{1.4} = (11.5 \pm 0.3) \frac{M}{M_\odot} \left(\frac{\tilde{\Lambda}}{800} \right)^{1/6} \text{ km.}$$

For GW170817, $M = 1.186 M_\odot$, $a' = 0.00375 \pm 0.00025$,

$$R_{1.4} = (13.4 \pm 0.1) \left(\frac{\tilde{\Lambda}}{800} \right)^{1/6} \text{ km.}$$

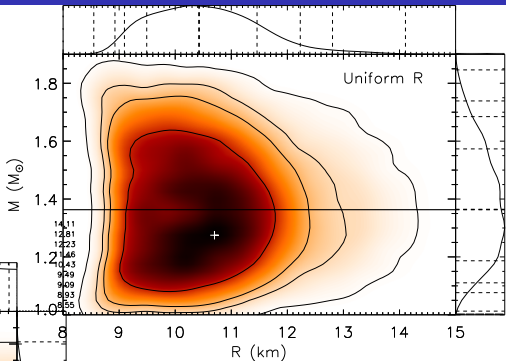
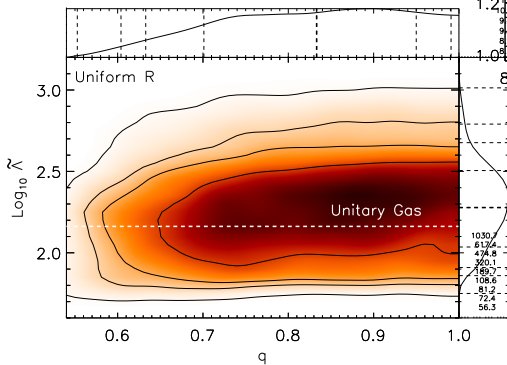
68.3%, 90%, 95.4% and 99.7% Confidence Bounds

Waveform analysis by De et al. (2018)

Zhao and Lattimer (2021)

Causality and uniform $\ln \Lambda$ priors

$$R = 10.4^{+1.1}_{-0.9} \text{ km}$$



$$\tilde{\Lambda} = 190^{+130}_{-81}$$

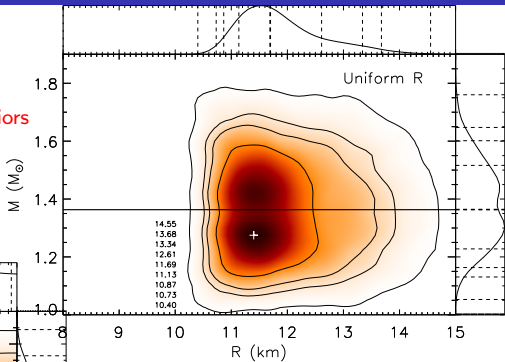
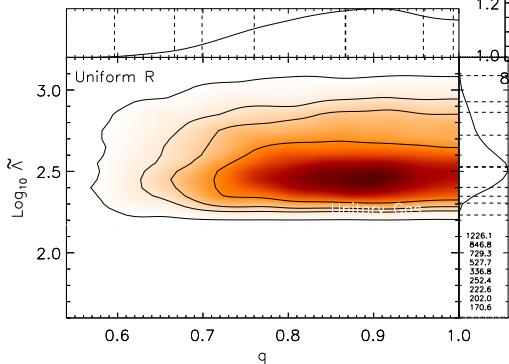
68.3%, 90%, 95.4% and 99.7% Confidence Bounds

Waveform analysis by De et al. (2018)

Zhao and Lattimer (2021)

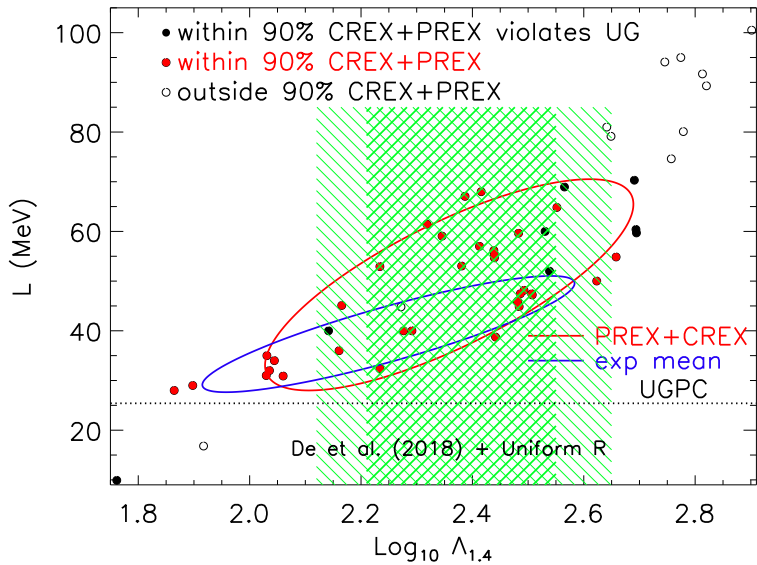
Unitary gas conjecture and uniform $\ln \Lambda$ priors

$$R = 11.7^{+0.9}_{-0.5} \text{ km}$$

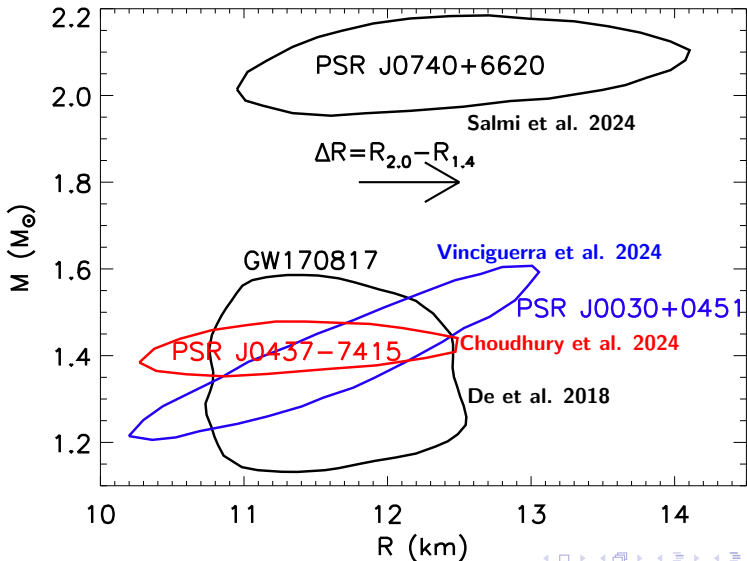


$$\tilde{\Lambda} = 337^{+191}_{-85}$$

Implied $\Lambda_{1.4} - L$

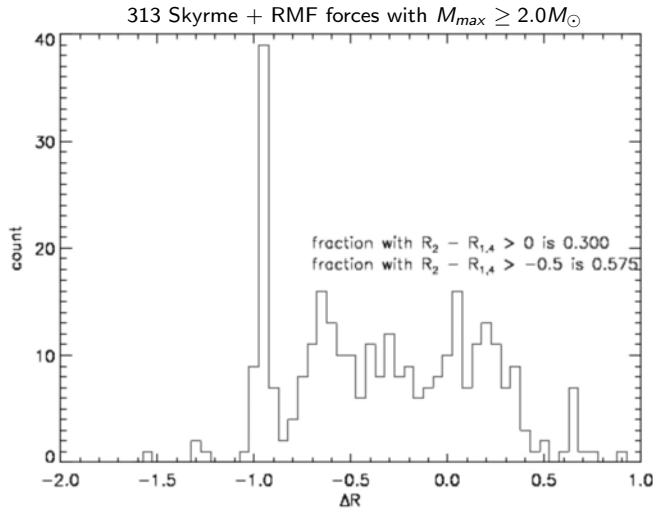


Summary of Astrophysical Observations



Importance of $\Delta R = R_{2.0} - R_{1.4}$

- ▶ • J0437-4715:
 $R = 11.36^{+0.95}_{-0.63}$ km
 - ▶ • J0740+6620:
 $R = 12.49^{+1.28}_{-0.88}$ km
- $\Delta R = 1.13^{+1.59}_{-1.08}$ km
- $\overline{\Delta R} = -0.25$ km



Moment of Inertia

- ▶ Spin-orbit coupling is of same order as post-post-Newtonian effects (Barker & O'Connell 1975, Damour & Schaeffer 1988).
- ▶ Precession alters orbital inclination angle (observable if system is face-on) and periastron advance (observable if system is edge-on).
- ▶ More EOS sensitive than R : $I \propto MR^2$.
- ▶ Measurement requires system to be extremely relativistic.
- ▶ Double pulsar PSR J0737-3037 is an edge-on candidate;
 $M_A = 1.338185^{+12}_{-14} M_\odot$.
- ▶ Even more relativistic systems are likely to be found, based on faintness and nearness of PSR J0737-3037. [PSR J0737-3039 ($P_b = 0.102$ d), PSR J1757-1854 (0.164 d), PSR J1946+2052 (0.078 d)]

Recent Moment of Inertia Measurement

